NATIONAL ADVISORY COMMITTEE FOR AERONAUTICS

WARTIME REPORT

ORIGINALLY ISSUED

April 1941 as
Advance Confidential Report

DESIGN OF NOZZLES FOR THE INDIVIDUAL CYLINDER EXHAUST JET PROPULSION SYSTEM

By Benjamin Pinkel, L. Richard Turner, and Fred Voss

Aircraft Engine Research Laboratory
Cleveland, Ohio

NACA

WASHINGTON

DESIGN OF NOZZLES FOR THE INDIVIDUAL CYLINDER EXHAUST JET PROPULSION SYSTEM

By Benjamin Pinkel, L. Richard Turner, and Fred Voss

SUMMARY

This report relates to the design of exhaust-stack nozzles for individual cylinder exhaust-gas jet propulsion and presents the results of tests on the effect of nozzle area on jet thrust and engine power. The tests were made on a single-cylinder engine mounted on a dynamometer stand.

A satisfactory method of correlating the test data for various engine-operating conditions is developed. Convenient curves are given for designing exhaust-stack nozzles and for predicting exhaust-gas thrust.

The thrust horsepower provided by the exhaust jet was found to be appreciable. An example calculated for the case of an airplane velocity of 350 miles per hour, altitude of 20,000 feet, and inlet manifold pressure of 45 inches Hg absolute, gave a value of exhaust jet thrust horsepower of 16 percent of the engine thrust horsepower.

INTRODUCTION

It has been shown by computation in reference 1, that an appreciable increase in net thrust horsepower might be expected on an aircraft engine when the exhaust stack of each of the engine cylinders is directed to discharge rearwardly. Flight tests on the XP-41 airplane (reference 2), showed that thrusts of the magnitude predicted by computation could be obtained in practice.

In the flight tests on the XP-41 airplane, two exhaust-stack nozzle sizes were tried and it was found that the

smaller nozzles gave larger jet thrust than the larger nozzles but, because the smaller nozzles introduced too great a restriction to the exhaust-gas flow, a loss in engine power occurred with the result that the net thrust horsepower and the maximum airplane velocity were greater for the larger nozzles. The maximum net thrust horsepower would probably have been obtained with an intermediate nozzle size. These tests indicated the need for data to determine the optimum exhaust nozzle size for maximum net thrust horsepower.

This report presents the results of tests made on a single-cylinder engine to determine the effect of exhaust-stack nozzle size on engine power and exhaust-gas thrust. The tests were made at the Langley Memorial Aeronautical Laboratory from July 1940 to March 1941.

SYMBOLS

A nozzle area, square feet

A_s exhaust stack area, square feet

A' nozzle area, square inches per cylinder

c_p specific heat at constant pressure of exhaust gas, foot-pounds per slug $^{\circ}F$

F average exhaust-gas thrust, pounds

F_θ instantaneous exhaust-gas thrust at crank angle θ, pounds

I indicated power, horsepower

I_o indicated power with an unrestricted exhaust stack, horsepower

I_c indicated power lost in the charging stroke, horsepower

M instantaneous mass flow of exhaust gas, slugs per second

M_e average mass flow of exhaust gas, slugs per second

m mass of exhaust gas already discharged at crank angle θ, slugs

m_a total mass of charge including residuals, slugs per cycle

m_e mass of fresh charge or exhaust gas, slugs per cycle

N engine speed, revolutions per second

N' engine speed, revolutions per minute

p_o atmospheric pressure, pounds per square foot, or inches Hg

p_a cylinder pressure at the time of exhaust-valve opening, pounds per square foot

$\bar{p}_d$ mean effective cylinder pressure during the discharge, pounds per square foot

p_e exhaust pressure, pounds per square foot

p_m intake manifold pressure, pounds per square foot or inches Hg

p_n nozzle pressure, pounds per square foot

p' total impact pressure in exhaust stack, pounds per square foot

P brake power, horsepower

P_o brake power with an unrestricted exhaust stack, horsepower

r volumetric compression ratio of engine

R gas constant of air, foot-pounds per slug $^{\circ}F$

R_e gas constant of exhaust gas, foot-pounds per slug $^{\circ}F$

T instantaneous temperature of exhaust gas in the cylinder, $^{\circ}F$ abs.

T_1 temperature of the fresh charge in the cylinder, $^{\circ}F$ abs.

T_a temperature of exhaust gas at the time of exhaust-valve opening, $^{\circ}F$ abs.

T_i standard intake air temperature, $^{\circ}F$ abs. (540° F abs.)

T_n instantaneous temperature of exhaust gas in the nozzle, °F abs.

T_s instantaneous temperature of exhaust gas in the exhaust stack, °F abs.

thp thrust power, horsepower

v volume, cubic feet

v_c clearance volume, cubic feet

v_d displacement volume, cubic feet

v_d' displacement volume, cubic inches per cylinder

V_c airplane velocity, feet per second

$\bar{V}_e$ mean exhaust-gas jet velocity, feet per second

V_n instantaneous velocity in the nozzle, feet per second

V_s instantaneous gas velocity in the exhaust stack, feet per second

γ ratio of specific heat of exhaust gas, 1.30

η_p propeller efficiency

η_t thermodynamic efficiency of the engine

η_v volumetric efficiency of the engine

θ crank angle, degrees or radians

θ_v duration of exhaust discharge process, radians

Ω weighting factor for exhaust-valve opening

ρ_a density of gas in the cylinder at the time of exhaust-valve opening, slugs per cubic foot

ρ_n density of gas in the nozzle, slugs per cubic foot

$$\phi = \frac{550\ I}{p_m\ v_d\ \frac{N}{2}} = \frac{imep}{p_m}$$

$$\phi_o = \frac{550\ I_o}{p_m\ v_d\ \frac{N}{2}}$$

$$\phi_c = \frac{550\ I_c}{p_m\ v_d\ \frac{N}{2}}$$

$$\Delta\phi = \phi - \phi_o$$

ANALYSIS

The gas in the cylinder at the end of the expansion stroke is at a pressure considerably above atmospheric and is capable of performing an appreciable amount of work by further expansion. Jet propulsion provides a means for utilizing this work. The potential energy in the cylinder is transformed into kinetic energy in the exhaust jet and thrust is derived from jet reaction.

In the conventional aircraft engine the gases are discharged through the valve passage with acoustic velocity, and considerable loss in the availability of the energy occurs because of acoustic shock and because the kinetic energy is transformed into heat by turbulence and friction in the bends and changes in passage area and shape. These losses can be reduced by providing nozzles at the end of the exhaust stacks. If an unlimited amount of time were available for the discharge process, then the use of nozzles having very small areas as compared with the valve-passage areas is obviously indicated, because then the velocity through the valve passages and exhaust ports would be very small with the result that the shock, friction, and turbulence losses would be minimized. The pressure would be transferred from the cylinder to the nozzle, where it may be efficiently converted into velocity. Because of the limited time actually available for discharge, operation with extremely small nozzles would result in the trapping of high-pressure exhaust gas in the engine and would cause a considerable loss in engine power. The optimum nozzle area is defined as that area which provides the maximum value for the sum of the engine and jet thrust horsepowers.

Because pressure ratios capable of providing supersonic velocities are involved, nozzles of the convergent-divergent type would theoretically give maximum efficiency. Nozzles of this type must be designed for a definite pressure ratio. The pressure in the exhaust stack varies cyclically with time, and for theoretical flow a nozzle with an exit area which also varies cyclically with time, would be required. A convergent-divergent nozzle which

does not vary with time would be little improvement over the simple convergent nozzle. The present report is concerned with the convergent nozzle.

The effects of nozzle area on engine power and exhaust thrust may be expected to be different for various engine conditions. In order to simplify the presentation of the data, to make the data available for more general application, and to reduce the number of tests, it is necessary to find the proper factors for correlating the data. Although the actual discharge process in an engine is complicated, the important factors may be revealed by a consideration of a simplified case provided the proper discharge phenomenon is chosen.

Effect of Nozzle Area on Engine Power

In the conventional aircraft engine with unrestricted stacks, the cylinder pressure may drop to atmospheric pressure during the exhaust event as early as 120 crank degrees before top center. As the discharge area of each stack is reduced by providing a nozzle, the discharge process is slowed down and the cylinder pressure is greater than atmospheric pressure for a larger part of the discharge period.

A small reduction in discharge area causes no noticeable effect on engine power but as the discharge area is further decreased, losses in engine power from two secondary sources become apparent successively, namely: (1) a loss in power caused by increased piston work against higher back pressures, and (2) a loss in power caused by the reduction in volumetric efficiency resulting from the presence of high-pressure exhaust gas in the cylinder during the valve-overlap period and at the time of closure of the exhaust valve. A range of nozzle sizes exists for which the first loss occurs but, because sufficient time is available for discharge of the cylinder pressure to atmospheric pressure before the opening of the intake valve, the second loss is not experienced. The second loss is accompanied by only a small additional reduction in economy.

The important variables that apply with regard to the effect of exhaust-stack nozzle area on engine power, are brought out by the following analysis. The indicated horsepower is the difference in indicated horsepowers of

the power process (compression and expansion strokes) and of the discharging and charging processes.

$$I = K M_e \eta_t - \frac{\bar{p}_d v_d N}{550 \times 2} - I_c$$

where

I indicated horsepower

M_e slugs of charge burned per second

η_t indicated thermal efficiency

K constant

$\bar{p}_d$ mean effective pressure during the discharge process

N engine revolutions per second

v_d engine displacement volume

I_c indicated power loss in charging process

If it is assumed that at the time the exhaust valve closes the clearance volume v_c of the engine is filled with gas at a pressure p_e, and if it is further assumed that during the charging process the residual gas in the clearance volume is compressed adiabatically to the inlet manifold pressure p_m, then the volume occupied by the residual gas is

$$v_c \left(\frac{p_e}{p_m}\right)^{1/\gamma}$$

and the volume remaining for inlet charge is

$$v = v_d + v_c - v_c \left(\frac{p_e}{p_m}\right)^{1/\gamma}$$

or

$$v = v_d \left[\frac{r}{r-1}\right]\left[1 - \frac{1}{r}\left(\frac{p_e}{p_m}\right)^{1/\gamma}\right] = v_d f_1 \left(\frac{p_e}{p_m}\right)$$

where r is compression ratio.

Thus for a given engine, the volume occupied by fresh charge is proportional to v_d and a function of p_e/p_m. The mass of fresh charge m_e occupying this volume is given by the gas law

$$m_e = \frac{p_m V}{RT_1} = \frac{p_m v_d}{RT_1} f_1\left(\frac{p_e}{p_m}\right)$$

where T_1 is the temperature of the fresh charge in the cylinder at the end of the intake stroke. But

$$W_e = m_e \frac{N}{2}$$

and

$$\text{imep} = \frac{550\ I}{v_d \frac{N}{2}}$$

Then

$$\phi = \frac{\text{imep}}{p_m} = \frac{550\ K}{R\ T_1} \eta_t\ f_1\left(\frac{p_e}{p_m}\right) - \frac{\bar{p}_d}{p_m} - \phi_c \qquad (1)$$

where

$$\phi_c = \frac{550\ I_c}{v_d\ p_m \frac{N}{2}}$$

If p_a is the cylinder pressure at the time the exhaust valve opens and T_a is the corresponding gas temperature, then consideration of the ideal Otto cycle indicates that p_a/p_m and T_a are constant for a constant inlet-charge temperature, fuel-air ratio, and p_c/p_m.

As a simplification, it is assumed that the nozzle presents the principal restriction to exhaust-gas flow in the range of present interest. The velocity of flow through the nozzle area A is proportional to the product of $\sqrt{T_a}$ and a definite function of p/p_o, where p is the variable pressure in the cylinder and p_o is atmospheric pressure. The volume rate at which gas leaves the cylinder at any pressure ratio p/p_o, is proportional to A. The rate at which cylinder volume is swept by the piston at any given crank angle is proportional to $v_d N$.

Thus for all cases in which the ratio of $v_d N$ to A is constant and p_a/p_o and T_a are also constant, p/p_o decreases in the same manner with crank angle and attains the same value p_e/p_o at valve-closing time. Thus p_e/p_o and $\overline{p}_d/p_o$ are functions of $\frac{v_d N}{A}$ and p_a/p_o at a constant value of T_a. However, for a constant air-fuel ratio and inlet-charge temperature the quantities p_a/p_m and T_a are constants; therefore, for these conditions p_e/p_o and $\overline{p}_d/p_o$ are functions of $\frac{v_d N}{A}$ and p_m/p_o only.

Equation (1) becomes:

$$\phi = \frac{imep}{p_m} = f_2\left(\frac{p_o}{p_m}, \frac{v_d N}{A}\right) - \phi_c \qquad (2)$$

To include the effect of variation in the value of T_a on the rate of discharge through the nozzle and to obtain a nondimensional expression, the factor $\frac{v_d N}{A}$ may be written $v_d N/A\sqrt{R_e T_a}$ where R_e is the constant in the gas law $p = \rho R_e T$. For the reason of simplicity of application and because T_a does not vary appreciably for a given fuel-air ratio, the factor $\frac{v_d N}{A}$ will be used in the present report.

Because of the change in thermal and volumetric efficiency with engine speed and because of the uncertainty in the value of the engine friction inherent in its determination from motoring runs, slightly different curves of ϕ against p_m/p_o and $\frac{v_d N}{A}$ may be expected for different engine speeds. To reduce the dispersion caused by engine speed for the purpose of more clearly defining the value of $\frac{v_d N}{A}$, at which the engine begins to lose power, the data are plotted as $\Delta\phi$ defined by

$$\Delta\phi = \phi - \phi_o = f_3\left(\frac{p_o}{p_m}, \frac{v_d N}{A}\right) \qquad (3)$$

where ϕ_o is the value which applies for the unrestricted exhaust stack at the same engine speed, inlet manifold

pressure and temperature, atmospheric pressure, and fuel-air ratio as that at which ϕ was determined. The quantity $\Delta\phi$ is a measure of the loss in power resulting from restriction of the exhaust-stack discharge area. Equation (3) indicates that the data on the effect of nozzle size on engine power may be correlated by plotting $\Delta\phi$ against p_m/p_o and $v_d N/A$.

Although the actual discharge process is complicated by additional phenomena, it is believed that the above discussion reveals the most important factors and is sufficiently accurate for the purpose at hand.

Effect of Nozzle Area on Exhaust Thrust

If it is assumed (1) that the largest part of the exhaust gas is discharged from the nozzle with acoustic velocity and (2) that there is an inappreciable loss in energy by heat transfer to the passage walls, then the following relations apply.

The thrust F_θ developed at the crank angle θ by the discharge of M slugs of gas per second at acoustic velocity is given by

$$F_\theta = V_n M + A (p_n - p_o)$$

where

V_n instantaneous velocity at the nozzle exit

p_n pressure in the exit of the nozzle

But

$$A p_n = \frac{M}{\rho_n V_n} p_n = M \frac{R_e T_n}{V_n}$$

where

T_n temperature at the nozzle exit

ρ_n density in the nozzle exit

Then

$$F_\theta = \left(V_n + \frac{R_e T_n}{V_n}\right) M - A p_o \qquad (4)$$

On the assumption that the energy lost by heat transfer to the walls is small, the equation for conservation of energy gives

$$c_p T = c_p T_n + \frac{1}{2} V_n^2 \qquad (5)$$

where T is the instantaneous temperature in the cylinder at crank angle θ. The well-known relation for acoustic velocity is

$$V_n = \sqrt{\gamma R_e T_n} \qquad (6)$$

Equations (5) and (6) give

$$V_n = \sqrt{2 \frac{R_e \gamma}{\gamma + 1} T}$$

and

$$T_n = T \frac{2}{\gamma + 1}$$

Equation (4) then becomes

$$F_\theta = \left(\frac{\gamma + 1}{\gamma}\right) M \sqrt{\frac{2 R_e \gamma}{\gamma + 1} T} - A p_o \qquad (7)$$

If T_a is the temperature in the cylinder at the time the exhaust valve opens, then on the assumptions that the piston work has only a small effect on the temperature of the largest part of the gas discharged and that the expansion in the cylinder is adiabatic

$$\frac{T}{T_a} = \left(\frac{\rho}{\rho_a}\right)^{\gamma-1} = \left(\frac{m_a - m}{m_a}\right)^{\gamma-1}$$

where

ρ instantaneous density in the cylinder at the crank angle θ

ρ_a density in the cylinder at the time the valve opens

m_a mass of exhaust gas in the cylinder at the time the exhaust valve opens

m mass of exhaust gas that has left the cylinder up to the crank angle θ

Equation (7) gives the instantaneous thrust at the time θ. If this thrust acts for an interval $d\theta$, then the average effect of this thrust over the complete cycle is

$$F_\theta \frac{d\theta}{4\pi} = \frac{\gamma+1}{\gamma} \sqrt{\frac{2 R_e \gamma}{\gamma+1} T_a} \left[1 - \frac{m}{m_a}\right]^{\frac{\gamma-1}{2}} \frac{M d\theta}{4\pi} - p_o A \frac{d\theta}{4\pi}$$

The total average thrust F is the summation of these average thrusts and is given by

$$F = \int_o^{\theta_v} \frac{F_\theta d\theta}{4\pi} = \frac{\gamma+1}{\gamma} \sqrt{\frac{2R_e\gamma}{\gamma+1} T_a} \int_o^{\theta_v} \left[1 - \frac{m}{m_a}\right]^{\frac{\gamma-1}{2}} \frac{M d\theta}{4\pi} - p_o A \frac{\theta_v}{4\pi}$$

where θ_v is the duration of the discharge process. But

$$\frac{M d\theta}{2\pi N} = dm$$

$$M_e = \frac{N m_e}{2}$$

where

m_e mass of exhaust gas discharged from the engine per cycle

and

M_e average rate of discharge of exhaust gas per second

Then

$$\int_o^{\theta_v} \left[1 - \frac{m}{m_a}\right]^{\frac{\gamma-1}{2}} \frac{M d\theta}{4\pi} = \frac{M_e}{m_e} \int_o^{m_e} \left[1 - \frac{m}{m_a}\right]^{\frac{\gamma-1}{2}} dm$$

$$= M_e \left(\frac{2}{\gamma+1}\right)\left(\frac{m_a}{m_e}\right) \left[1 - \left(1 - \frac{m_e}{m_a}\right)^{\frac{\gamma+1}{2}}\right]$$

$$\frac{F}{M_e} = \frac{2}{\gamma} \sqrt{\frac{2R_e\gamma}{\gamma+1} T_a} \frac{m_e}{m_a} \left[1 - \left(1 - \frac{m_e}{m_a}\right)^{\frac{\gamma+1}{2}}\right] - \frac{p_o A}{M_e} \frac{\theta_v}{4\pi} \qquad (8)$$

It was previously pointed out that for a given engine, operating at a given air-fuel ratio and inlet-air temperature, the temperature T_a is substantially constant.

The quantity $\frac{n_a}{n_e}\left[1-\left(1-\frac{n_e}{n_a}\right)^{\frac{\gamma+1}{2}}\right]$ is close to unity in value and varies only slightly with operating conditions. Therefore F/M_e is a function principally of $\theta_v p_o A/M_e$. The quantity F/M_e, which is the thrust per unit mass of exhaust-gas flow per second, will be represented by the symbol $\overline{V}_e$ and will be called the average effective exhaust-gas jet velocity.

It has been shown in the previous section that the pressure ratio p/p_o during the discharge period varies substantially in the same manner with crank angle for all cases for which p_o/p_m and $v_d N/A$ are constant. Thus the discharge period θ_v is a function of p_o/p_m and $v_d N/A$.

$$\theta_v = f_4\left(\frac{p_o}{p_m}, \frac{v_d N}{A}\right)$$

As $v_d N/A$ increases or p_o/p_m decreases, θ_v approaches the crank-angle duration that the exhaust valve is open. Therefore, in the range where $v_d N/A$ is large or p_o/p_m is small, F/M_e in equation (8) when plotted against $p_o A/M_e$ approaches a straight line, the slope of which is $-\theta_v/4\pi$ where θ_v becomes the crank-angle duration that the exhaust valve is open.

The quantity $v_d N/A$ is equal to

$$\frac{v_d N}{A} = \frac{p_o}{p_m}\frac{M_e}{A p_o}\left(\frac{2RT_i}{\eta_v}\right)\left(\frac{1}{(1+f)}\right)$$

where f is the fuel-air ratio.
For a constant value of $p_o A/M_e$, an increase in p_o/p_m results in an increase in $v_d N/A$. But increases in the values of p_o/p_m and $v_d N/A$ have opposite effects on the value of θ_v. Thus it is expected that the effect of variation of p_o/p_m on θ_v for a constant value of $p_o A/M_e$

is small and that θ_v depends mainly on $p_o A/M_e$. It is therefore believed that over the largest part of the interesting range F/M_e is a function principally of $p_o A/M_e$. The test data will be presented by plotting F/M_e against $p_o A/M_e$ and will be examined for trends with respect to p_o/p_m.

The above analysis is admittedly approximate as it assumes acoustic velocity at the exhaust nozzle over the entire discharge process, neglects heat transfer to the walls and neglects the contribution of the piston work toward raising the temperature in the cylinder. Its principal virtue is that it points out the important variable on which the thrust depends. A somewhat more exact analysis, in which the first assumption is not made, is given in appendix I.

The thrust horsepower of the exhaust-gas jet is given by

$$thp = V_o M_e \frac{\overline{V}_e}{550}$$

when V_o is airplane velocity in feet per second.

APPARATUS

The single-cylinder test engine for this investigation was a Wright 1820-G engine modified to operate with only one cylinder. The regular crankcase, crankshaft, cams, piston, and master connecting rod were retained. The compression ratio was 6.4:1. The exhaust valve timing and lift diagram are shown in figure 12. The air-cooled cylinder was enclosed in a sheet-metal jacket open at the front and rear and a motor-driven centrifugal blower provided the necessary cooling air. High-pressure air for the supercharged condition was obtained from the central air supply. An electric dynamometer was used to measure the torque of the engine, and an electrically operated revolution counter and a stop watch for determining the engine speed. Thermocouples were provided to measure cylinder temperatures. The engine air charge was measured by means of an orifice plate in the air-intake pipe. A tank was installed between the engine and the orifice plate to damp out pulsations. The fuel-flow rate was measured by a rotameter.

The exhaust stack was a straight pipe $2\frac{5}{16}$ inches inner diameter and 20 inches long. One end of the exhaust stack was provided with a flange for the attachment of various exit nozzles. The nozzles used had a uniform length of 5 inches and consisted of a 3-inch tapered section having a 1-inch straight section on each end. Smooth transitions from the tapered to straight sections were provided. The exhaust gases were discharged into a tank or into one or two thrust-measuring devices and removed by an exhauster.

The tank which was used during the tests to determine the effect of exhaust-nozzle restriction on engine power with various exhaust pressures, had a volume of approximately 70 cubic feet. The exhaust pipe was connected to the tank with a length of flexible tubing. A tap for measuring static pressure was located in the tank.

The mean exhaust-gas thrust at sea-level exhaust pressure was measured by means of the thrust target shown diagrammatically in figure 1(a). The exhaust gas discharged from the nozzle B entered the target through the hole in the cover plate A, impinged on the stainless-steel plate C, and left the target through the two pipes D normal to the jet and parallel to the axis of support of the target. These pipes were provided with vertical guide vanes, E, to insure discharge of the gas from the tank in a direction normal to the nozzle axis. The exhaust manifold F fitted over these pipes but without contact. The hole in the cover plate A was approximately 3/8 inch greater in diameter than the nozzle exit passage. A different plate was used for each nozzle size. The end of the nozzle was located approximately 1/4 inch from the plate A. Pressure tap M was located in the target in a position to measure static pressure only. The edge of the tap was rounded to avoid errors otherwise introduced by the fluctuations in pressure.

Exhaust-gas thrust measurements at simulated altitude conditions were made by means of the thrust target shown in figure 1(b). The target K was suspended within the tank L which was connected to the blower. Altitude pressures could be maintained in the tank by operation of the blower. The nozzle B was attached to the tank L in a manner to prevent leakage. The exhaust gas entered the target through the hole in the cover plate A. As in the previous case, a separate cover plate was provided for each nozzle. Deflectors C were provided to distribute the ex-

haust gas in the target and guide vanes E to insure discharge of the exhaust gas through exit pipe D in a direction perpendicular to the nozzle axis. The axis of the pipe D intersected the axis of the hollow shaft O in order to minimize torsional reaction to the discharge of exhaust gas from the target. Water was circulated through the hollow shaft O for cooling. Static pressure taps P and Q were located in the target and tank, respectively. The pressure was transmitted from tap P through a thin tube R coiled to provide a negligible restraining force on the target. The pressure taps were rounded at their edges and connected to tubes of small diameter (0.040 in. I.D.) in order to obtain correct averages of the fluctuating pressures. The pressures were measured by means of manometers.

Both of the targets were supported on ball bearings G. The exhaust thrust was determined from readings of the platform scales H (fig. 1(a)) and the moment arms. To overcome vibration, the load on the scales was increased by weights I and carried on rubber bushings J.

Photographs of the two thrust devices set up on the test engine are shown in figures 2(a) and (b).

Army 100 octane fuel was used in these tests.

METHODS

Effect of Nozzle Area on Engine Power

The effect of exhaust restriction on engine power was determined at the engine speeds of 1300, 1500, 1700, 1900, and 2100 rpm and at maximum power fuel-air ratio, 0.08. Variation in speed of ±10 rpm and of fuel-air ratio from 0.079 to 0.081 was permitted. In general, for each exhaust nozzle the engine was operated at each speed over the following range of conditions:

(a) Inlet manifold pressure 30 inches Hg abs. and exhaust tank pressures varied from 12 to 30 inches Hg abs.

(b) Inlet manifold pressure varied from 24 to 30 inches Hg abs. and exhaust tank pressure constant at 30 inches Hg.

In addition, variable manifold pressure runs at boosts up to 36 inches Hg abs. were made with the target shown in figure 1(a).

The nozzle areas tested were 0.91, 1.29, 1.39, 1.77, 2.85, and 4.20 square inches.

In all tests the oil-out temperature was held between 140° and 160° F and the cooling-air pressure drop was held at approximately 20 inches H_2O. The carburetor inlet temperature remained at approximately 80° F, the maximum variation ±10° F. The engine power and charge-air consumption were corrected to a carburetor air temperature of 80°F on the assumption that they vary inversely as the square root of the absolute temperature.

Motoring friction with the unrestricted exhaust stack was measured at each speed with sea-level inlet and exhaust pressure. These values were plotted against engine speed and the data faired. The friction determined from the faired curve was used for all nozzles to compute the indicated mean effective pressure. The ratio of the indicated mean effective pressure to inlet manifold pressure ϕ is plotted against the ratio of exhaust tank pressure to inlet manifold pressure p_o/p_m in figure 3.

The volumetric efficiency η_v was calculated from the corrected weight of charge air by means of the following relation:

$$\eta_v = \frac{2 R T_i}{v_d N p_m} \times \text{mass of charge air per second}$$

where T_i is the standard carburetor air temperature (80° F + 460° F in this case). The volumetric efficiency is shown in figure 4 plotted against p_o/p_m.

The quantity $\Delta\phi$ for each nozzle was taken as the difference between the value of ϕ for that nozzle and for the unrestricted exhaust stack at the same values of engine speed and p_o/p_m. The values of $\Delta\phi$ were calculated from the faired curves in figure 3 and are shown in figure 5 plotted against v_dN/A for constant values of p_o/p_m as suggested by equation (3) and the discussion in the section on analysis.

The quantity $\Delta\eta_v$ was determined from figure 4 in a manner similar to that described for $\Delta\phi$ and is shown in figure 6. The values of $\Delta\phi$ and $\Delta\eta_v$ at $p_o/p_m = 0.2$, were obtained by extrapolating the curves in figures 3 and 4. The lines through the points in figure 5 were established by the method of least squares. The points at which the oblique lines intersect the $\Delta\phi = 0$ lines define critical values of v_dN/A. The critical values of v_dN/A are plotted in figure 7 against p_o/p_m and are designated by $\Delta\phi = 0$. The values of v_dN/A at which $\Delta\phi = -0.5$ and -1.0, are also shown in this figure.

Effect of Nozzle Area on Exhaust Thrust

The effect of nozzle size on exhaust thrust was determined for the following range of engine conditions:

Nozzle area sq in.	Engine speed, rpm 1300		1500		1700		1900		2100	
	p_m	p_o	p_m	p_o	p_m	p_o	p_m	p_o	p_m	p_o
0.91	v	30	v	30	v	30	v	30	v	30
			30	v					30	v
1.39	v	30			v	30			v	30
1.77	v	30	v	30	v	30	v	30	v	30
			30	v						
			35	v						
2.85	v	30	v	30	v	30	v	30	v	30
4.20	v	30			v	30			v	30

The symbol v in a column headed p_m indicates that the manifold pressure was varied over a range from 22 to 36 inches Hg absolute, while the same symbol in a column headed p_o indicates that the exhaust discharge pressure was varied from 12 to 30 inches Hg absolute. All tests were made with the target shown in figure 1(a) except those marked variable p_o, which were made with the target shown in figure 1(b).

The thrust of the exhaust gas was determined by discharging the exhaust gas into the targets shown in figure 1 and by reading on the scale a quantity proportional to the reaction of the target. Because each target is designed to discharge the exhaust gas at right angles to the direction that it issues from the exhaust stack, the reaction of the target is equal to the exhaust-gas thrust. The target reaction was calculated from the scale reading by multiplying by the lever-arm ratio.

The weight of exhaust gas was determined by means of the calibrated orifice in the air-intake line and the rotameter in the fuel line. The thrust data are presented by plotting the ratio F/M_e or $\bar{V}_e$ against $p_o A/M_e$ in accordance with equation (8) and the associated discussion in the analysis. A separate plot of the data for each nozzle is shown in figure 9. All the data taken have been collected in figure 10.

Indicator cards were taken in the cylinder and exhaust stack by means of the Farnboro indicator at an engine speed of 1900 rpm and sea-level inlet manifold and exhaust pressure for the following nozzle areas 0.91, 1.39, 1.77, 2.24, 2.85, and 4.20 square inches.

The impact pressure in the exhaust stack and the instantaneous and average thrust were calculated by the method given in appendix II. The pressure in the cylinder and exhaust stack, and the instantaneous thrust and mass flow of exhaust gas are plotted in figure 12.

The mean exhaust-gas jet velocity calculated from the indicator cards is plotted with other data in figure 9.

The maximum cylinder-head temperature for various nozzles is shown in figure 13. These temperatures were corrected to a common cooling air inlet temperature by means of the assumption that a 1° change in cooling air inlet temperature caused 0.8° change in the head temperature.

DISCUSSION OF RESULTS

The Effect of Nozzle Size on Engine Power

The variation with p_o/p_m of $imep/p_m$ and volumetric efficiency for a range of nozzle sizes and engine speeds is

shown in figures 3 and 4, respectively. The value of p_o/p_m was varied by changing the values of p_o and p_m. The same curve is obtained for a given nozzle and engine speed regardless of which of the terms in the quantity p_o/p_m is varied. This result is in agreement with the analysis and equation (2). The curves marked 4.20-square-inch nozzle area represent the unrestricted exhaust-stack condition. The quantity $\Delta\phi$, which represents the loss in specific indicated mean effective pressure resulting from a reduction in nozzle size, is obtained by subtracting the values of $imep/p_m$ for a given nozzle from the values for the unrestricted stack at the same engine speeds and the same values of p_o/p_m. The quantity $\Delta\phi$ is seen in equation (3) to be a function of p_o/p_m and v_dN/A. The values of $\Delta\phi$ obtained from figure 3 are shown in figure 5 plotted against v_dN/A for various values of p_o/p_m. It is noted that a single curve is obtained when $\Delta\phi$ is plotted against v_dN/A regardless of whether engine speed or nozzle size is varied. This is further substantiation that the analysis leading up to equation (3) reveals the correct primary variables. Figure 6 shows a similar plot of $\Delta\eta_v$ against v_dN/A and p_o/p_m obtained from figure 4.

It is noted in figure 5 that at low values of v_dN/A, $\Delta\phi = 0$ but that as v_dN/A is increased a point is reached where $\Delta\phi$ decreases sharply with further increase in v_dN/A. Although a smooth transition from the region $\Delta\phi = 0$ to the region of loss in power probably occurs, the transition is so sharp that no appreciable error results from drawing separate straight lines through the points in the two regions. The intersection of these lines marks the critical value of v_dN/A.

The curve in figure 7 labeled $\Delta\phi = 0$ is a plot of the critical values of v_dN/A against p_o/p_m obtained from figure 5. Curves are also given for $\Delta\phi = -0.5$ and -1.0.

A comparison of figures 5 and 6 shows, as nozzle size is reduced for a given set of operating conditions, that the point at which power loss begins is reached before the engine loses volumetric efficiency. The difference is caused by the increase in piston work with reduction in nozzle size which becomes noticeable before loss in volumetric efficiency.

The curves shown in figure 7 are applicable to other engines having a similar valve timing and ratio of valve-passage area to cylinder volume regardless of the cylinder displacement volume. It is believed that present-day engines are sufficiently similar in design to permit use of these data on most of these engines. If the exhaust valve in a particular engine opens appreciably earlier or closes appreciably later than that on the engine tested, the nozzle sizes calculated for this engine from figure 7 are conservative while for engines having an appreciably later valve-opening time or earlier valve-closing time, the nozzles predicted from figure 7 may result in some loss in engine power.

The present data relate to a fuel-air ratio of 0.08. For operation at other fuel-air ratios, some deviation from the results shown in figure 7 may be expected. In the analysis it was predicted that for constant p_a/p_o there should be flow similarity for constant $v_d N/A\sqrt{R_e T_a}$. The critical value of $v_d N/A$ for a fuel-air ratio of 0.08 does not change much with p_o/p_m, and hence would not change much with p_a/p_o. For mixtures giving lower values of T_a, the critical value of $v_d N/A$ would be expected to decrease in proportion to the square root of $R_e T_a$.

In the flight tests with a Pratt & Whitney 1830 engine, reported in reference 2, a loss in ϕ of 0.86 was obtained with the smaller nozzle (1.77 sq in.) at a value of p_o/p_m of 0.305 and a value of $v_d N/A$ of 261 feet per second. A point is plotted in figure 7 at these values of p_o/p_m and $v_d N/A$, and indicates that the value of $\Delta\phi$ observed checks very closely with that given by figure 7. Computations on the larger nozzle used in these tests showed that this nozzle operated at a value of $v_d N/A$ of 135 feet per second, which is less than critical value and it may be concluded that a somewhat larger thrust could have been obtained with no loss in engine power by using a nozzle size intermediate to the two tested.

It is shown in appendix III that when a reduction in nozzle area results in a loss in engine power, the loss in engine thrust horsepower will be greater than the gain in exhaust-jet thrust horsepower obtained by this change in nozzle area. Thus the curve $\phi = 0$ in figure 7 defines the optimum nozzle area. This curve is represented by the nomogram in figure 8.

The nozzle area is obtained from the nomogram by (1) joining the values of v_d' and N' with a straight edge, (2) marking the intersection of the straight edge with the reference line, and (3) drawing a straight line through this intersection and the value of p_o/p_m. The intersection of this line with the A' scale gives the required nozzle area. An example is shown on the nomogram in which v_d' = 202 cubic inches per cylinder, N' = 2300 rpm, and p_o/p_m = 0.3. The nozzle area obtained for this case is 3.56 square inches per cylinder.

The slopes of the curves in figure 5 at the values of v_dN/A above the critical value are designated by $-d(\Delta\phi)/d(v_dN/A)$ and are shown in figure 7 plotted against p_o/p_m.

Effect of Nozzle Size on Exhaust Thrust

The data on the effect of nozzle size on exhaust-gas thrust are shown in figures 9 and 10, in which the thrust as represented by F/M_e or $\bar{V}_e$ is plotted against p_oA/M_e. The points for each nozzle area are plotted on separate curves in figure 9 and are coded according to engine speed and to inlet and exhaust conditions in order to allow examination of the data for any trend with respect to these variables. The curves in figure 9 are sections of the curve in figure 10.

The dispersion of the points in figure 9 appears to be the result mainly of experimental error as no trend can be noticed with the variables mentioned. All the data are plotted as a single curve in figure 10. It may be concluded from an examination of this figure that plotting $\bar{V}_e$ against p_oA/M_e provides good correlation of the data over the complete range of operating conditions. The correlation is somewhat better at the lower values of p_oA/M_e as was expected from the discussion in the analysis.

In the section on the effect of nozzle size on engine power, a method was given for determining the nozzle size when the engine-operating conditions are known. With this value of nozzle size and the values of atmospheric pressure and the mass of exhaust gas discharged per second, the value of p_oA/M_e can be calculated. The value of $\bar{V}_e$ can then be obtained from figure 10 corresponding to this value of

$p_o A/M_e$, and the exhaust thrust and thrust horsepower may be calculated from

$$F = M_e \bar{V}_e$$

$$thp = M_e \bar{V}_e V_o/550$$

For example, if the conditions of the example in the previous section are assumed and if in addition the atmospheric pressure p_o (20,400 ft altitude) is 960 pounds per square foot and the engine power per cylinder is 100 horsepower, then on the assumption of 0.002 pound of exhaust gas per second per brake horsepower, the thrust is obtained as follows:

$$\frac{p_o A}{M_e} = 960 \times \frac{3.56}{144} \times \frac{32.2}{0.2} = 3820 \text{ feet per second}$$

From figure 10 for this value of $p_o A/M_e$

$$\bar{V}_e = 2320 \text{ feet per second}$$

The thrust is

$$F = 2320 \times \frac{0.2}{32.2} = 14.4 \text{ pounds per cylinder}$$

At an airplane velocity of 350 miles per hour (513 ft per sec), the thrust horsepower is

$$thp = 14.4 \times \frac{513}{550} = 13.4 \text{ hp per cylinder}$$

On the assumption of a propeller efficiency of 85 percent, this thrust horsepower is 16 percent of the engine thrust horsepower.

A more extended example of the gain in thrust horsepower to be expected from exhaust-gas jet propulsion is shown in figure 11. In these computations an inlet manifold temperature of 80° F, an exhaust-gas flow of 0.002 pound per second per brake horsepower, a propeller efficiency of 0.85, and the volumetric efficiency shown for the unrestricted stack in figure 4(c) were assumed.

Effect of Exhaust Stack Nozzle Area on the Exhaust Process

The static pressures in the cylinder and exhaust stack measured by means of a Farnboro indicator are shown in figure 12 for a series of nozzle sizes and the following engine conditions:

Engine speed	1900 rpm
Inlet manifold pressure	30 in. Hg
Atmospheric pressure	30 in. Hg
Fuel-air ratio	0.08

The impact pressure in the exhaust stack, calculated by means of equations developed in appendix II, is also shown in this figure. The impact pressure for the large nozzles is considerably less than the cylinder pressure, showing a large loss in available mechanical energy through the exhaust port. As the nozzle size is decreased, the impact pressure in the stack approaches the cylinder pressure and the loss in available mechanical energy is decreased. The increase in available mechanical energy results in an increase in exhaust thrust. The values of the exhaust thrust, calculated from the impact pressures and determined from the experimental data in figure 10, are given in figure 12 and are seen to be in fair agreement. It is noted that although the exhaust thrust increases continuously with reduction in nozzle area, the value of ϕ remains substantially constant until a nozzle area between 2.24 and 1.77 square inches is reached, beyond which further reduction in nozzle area causes a large decrease in power. Figure 7 shows that the maximum value of $v_d N/A$ for no loss in engine power for $p_o/p_m = 1$ is 250 feet per second. This value of $v_d N/A$ lies between the values for the 2.24 and 1.77-square-inch nozzles. (See fig. 12.)

The exhaust and inlet valve lift diagrams (cold) are shown in figure 12. A line is drawn at a lift equal to the additional exhaust-valve clearance for the hot engine. The intersections of this line with the cold exhaust-valve lift diagram indicate the positions of exhaust-valve opening and closing. The valve clearance was obtained for the

hot condition by quickly shutting down the engine after a power run and measuring the clearance as soon as possible. Because of the delay inherent in this method, some error might be expected in this determination of valve clearance.

Effect of Nozzle Area on Engine Temperatures

Temperatures were measured on the cylinder head at the rear spark-plug gasket, a point on the cylinder head near the rear spark plug, a point between the exhaust port and the rear spark plug, and at the rear of the barrel. The point between the rear spark plug and the exhaust port had the highest temperature. This temperature is plotted against A and p_o/p_m in figure 13 for p_m = 30 inches of mercury absolute and three engine speeds 1300, 1500, and 2100 rpm. Plotted on this figure are also the critical nozzle areas determined from figure 7. It is noted that for nozzle areas greater than the critical area, only a small increase in temperature results from decrease in nozzle area. A marked increase in head temperature with reduction in nozzle area below the critical area is noted. This increase in temperature occurs in spite of the reduction in engine power resulting from operation with nozzle areas less than critical and is attributed to the fact that exhaust gas is maintained within the engine port and cylinder for a larger part of the cycle, and that the larger quantity of exhaust gas trapped in the cylinder results in larger average gas temperatures.

CONCLUSIONS

1. As the discharge areas of the exhaust stacks are reduced, the exhaust-gas jet thrust per unit mass per second of exhaust gas is increased.

2. Above a critical nozzle area, reduction in nozzle area results in a negligible reduction in engine power. Below the critical nozzle area, reduction in nozzle area results in a sharp reduction in engine power.

3. At nozzle areas less than the critical area, the loss in engine power is much greater than the gain in exhaust-gas jet thrust horsepower for airplane velocities considerably in excess of present-day velocities. Thus,

operation at the critical nozzle area provides the maximum net-thrust horsepower.

4. The value of the critical nozzle area depends on the engine-operating conditions. The data on critical nozzle area may be correlated by plotting the factor displacement volume × engine speed ÷ nozzle area against the ratio of atmospheric pressure to inlet manifold pressure.

5. The data on exhaust-gas jet thrust may be correlated by plotting the factor thrust ÷ mass of exhaust gas discharged per unit time against the factor atmospheric pressure × nozzle area ÷ mass of exhaust gas discharged per unit time.

6. The thrust horsepower provided by the exhaust jet was found to be appreciable. An example calculated for the case of an airplane speed of 350 miles per hour, altitude of 20,000 feet, and inlet manifold pressure of 45 inches of mercury absolute gave a value for the exhaust-gas jet thrust horsepower of 16 percent of the engine thrust horsepower.

Langley Memorial Aeronautical Laboratory,
National Advisory Committee for Aeronautics,
Langley Field, Va.

REFERENCES

1. Oestrich, Hermann: Prospects for Jet Propulsion of Airplanes with Special Reference to Exhaust Gases. Misc. Paper No. 34, NACA, 1932.

2. Pinkel, Benjamin, and Turner, L. Richard: Flight tests of Exhaust Gas Jet Propulsion. NACA confidential report, 1940.

APPENDIX I

Intermittent Discharge of Exhaust Gas Through a Convergent Nozzle

The instantaneous thrust, F_θ, produced by a stream of exhaust gas flowing from a nozzle is given by

$$F_\theta = MV_n + p_nA - p_oA \tag{9}$$

The mass flow M is given by

$$M = \rho_n A V_n \tag{10}$$

where

$$\rho_n = p_n/R_eT_n$$

and the velocity V_n is given by

$$V_n = \sqrt{2J\ c_p(T - T_n)} \tag{11}$$

where T is the total temperature of the gas upon being brought to rest adiabatically.

When equations (10) and (11) are substituted in (9),

$$F_\theta = p_nA\left[\frac{2\gamma}{\gamma - 1}\left(\frac{T}{T_n} - 1\right) + 1\right] - p_oA \tag{12}$$

Addition and subtraction of the term

$$\frac{\gamma + 1}{\gamma} M \sqrt{\frac{2\gamma R_eT}{\gamma + 1}}$$

gives

$$F_\theta = \frac{\gamma + 1}{\gamma} M \sqrt{\frac{2\gamma R_eT}{\gamma + 1}} + p_nA\left[\frac{2\gamma}{\gamma + 1}\left(\frac{T}{T_n} - 1\right) + 1\right]$$

$$- p_oA - \frac{\gamma + 1}{\gamma} M \sqrt{\frac{2\gamma R_eT}{\gamma + 1}} \tag{13}$$

When the value of M from (10) and (11) is substituted in (13)

$$F_\theta = \frac{\gamma + 1}{\gamma} M \sqrt{\frac{2\gamma R_e T}{\gamma + 1}} - p_o A \left\{ \frac{p_n}{p_o} \left[2 \sqrt{\frac{\gamma + 1}{\gamma - 1} \frac{T}{T_n} \left(\frac{T}{T_n} - 1 \right)} - \frac{2\gamma}{\gamma - 1} \left(\frac{T}{T_n} - 1 \right) - 1 \right] + 1 \right\} \qquad (14)$$

Integration over a complete cycle and division by the average mass flow of exhaust gas, M_e, gives:

$$\overline{V}_e = \frac{F}{M_e} = \int_0^{4\pi} \frac{F_\theta}{M_e} \frac{d\theta}{4\pi} = \sqrt{\frac{2(\gamma + 1)}{\gamma}} \int_0^{4\pi} \frac{M}{M_e} \sqrt{R_e T} \frac{d\theta}{4\pi}$$

$$- \frac{p_o A}{M_e} \int_0^{4\pi} \left\{ \frac{p_n}{p_o} \left[2 \sqrt{\frac{\gamma + 1}{\gamma - 1} \frac{T}{T_n} \left(\frac{T}{T_n} - 1 \right)} - \left(\frac{2\gamma}{\gamma - 1} \right) \left(\frac{T}{T_n} - 1 \right) - 1 \right] + 1 \right\} \frac{d\theta}{4\pi} \qquad (15)$$

For isentropic flow through a convergent nozzle at the critical pressure ratio $p_n \geqq p_o$ the ratio T/T_n is equal to $\frac{\gamma + 1}{2}$ and the term

$$2 \sqrt{\frac{\gamma + 1}{\gamma - 1} \frac{T}{T_n} \left(\frac{T}{T_n} - 1 \right)} - \frac{2\gamma}{\gamma - 1} \left(\frac{T}{T_n} - 1 \right) - 1$$

vanishes. Thus the integrand, Ω, given by

$$\Omega = \frac{p_n}{p_o} \left[2 \sqrt{\frac{\gamma + 1}{\gamma - 1} \frac{T}{T_n} \left(\frac{T}{T_n} - 1 \right)} - \frac{2\gamma}{\gamma - 1} \left(\frac{T}{T_n} - 1 \right) - 1 \right] + 1$$

is equal to unity when the flow of exhaust gas is critical. At other pressure ratios, when the discharge velocity is less than the critical velocity, $p_n = p_o$. The value of Ω for this condition may be found as a function of the ratio of atmospheric pressure to the total exhaust-stack impact pressure from the relationship connecting pressure

and temperature for isentropic expansion, namely,

$$\frac{T}{T_n} = \left(\frac{p'}{p_o}\right)^{\frac{\gamma-1}{\gamma}} \tag{16}$$

where p' is the total stack pressure including the velocity head. The function Ω is displayed in figure 14. Its value is nearly unity for all but low values pf p'/p_o and it has the value zero when the exhaust valve is closed. Ω thus represents a weighting factor for the time of exhaust discharge. When the mass flow per unit area is large or the discharge pressure is low, the stack pressure is appreciably greater than atmospheric pressure for most of the time while the valve is open, and Ω is nearly unity for all of this time. Hence for small values of $p_c A/M_e$ the integral

$$\int_0^{4\pi} \Omega \frac{d\theta}{4\pi} \longrightarrow \frac{\theta_v}{4\pi}$$

The approximate value of the integral

$$\int_0^{4\pi} \frac{M}{M_o} \sqrt{R_c T}$$

was shown in the section on analysis, to be given by

$$\int_0^{4\pi} \frac{M}{M_e} \sqrt{R_e T} = \frac{2}{\gamma + 1} \frac{n_a}{n_e} \left[1 - \left(1 - \frac{n_e}{n_a}\right)^{\frac{\gamma+1}{2}}\right] \sqrt{R_e T_a}$$

The variation of

$$\frac{n_a}{n_e} \left[1 - \left(1 - \frac{n_e}{n_a}\right)^{\frac{\gamma+1}{2}}\right]$$

with n_e/n_a is displayed in figure 14. Its value is very

nearly unity for all practical values of m_e/m_a. On the assumption that this function and Ω are both unity, equation (15) becomes

$$\bar{v}_e \longrightarrow \frac{2}{\gamma}\sqrt{\frac{\gamma}{\gamma+1}R_e T_a} - \frac{p_o A}{M_e}\frac{\theta_v}{4\pi}$$

Equation (12) may be rewritten in terms of the pressure ratio p'/p_o to provide a means of calculating the exhaust-gas thrust from pressure records. In the region where the flow is critical, T/T_n and p'/p_n are functions of γ and F_θ is given by

$$F_\theta = p_o A\left[\frac{p'}{p_o}\,2\left(\frac{2}{\gamma+1}\right)^{\frac{1}{\gamma-1}} - 1\right] \qquad (17)$$

In the region where the flow velocity is less than acoustic, $p_n = p_o$ and F_θ is given by

$$F_\theta = p_o A\,2\,\frac{\gamma}{\gamma-1}\left[\left(\frac{p'}{p_o}\right)^{\frac{\gamma-1}{\gamma}} - 1\right] \qquad (18)$$

These relations were used to calculate the thrust from the indicator cards. The method used to determine p'/p_o is described in appendix II.

APPENDIX II

Calculation of Exhaust Gas Thrust from Indicator Diagrams

The ideal thrust produced by a convergent nozzle may be calculated by means of equations (17) and (18) (appendix I) if the total pressure, p', in the nozzle is known. The pressure ordinarily measured is the static pressure which must be corrected for the approach velocity. The total pressure may be calculated as follows:

From the continuity condition

$$\frac{p_s A_s V_s}{R_c T_s} = \frac{p_n A V_n}{R_c T_n}$$

where

A_s stack area

p_s stack pressure

V_s corresponding velocity

T_s corresponding temperature

If it is assumed that no heat is lost from the stack to the nozzle, the principle of the conservation of energy gives:

$$V_s^2 = (T - T_s) \frac{2\gamma}{\gamma - 1} R_c$$

$$V_n^2 = (T - T_n) \frac{2\gamma}{\gamma - 1} R_c$$

The continuity equation becomes

$$\frac{p_s A_s \sqrt{T - T_s}}{T_s} = p_n A \frac{\sqrt{T - T_n}}{T_n}$$

But

$$\frac{T_s}{T} = \left(\frac{p_s}{p'}\right)^{\frac{\gamma-1}{\gamma}}$$

and

$$\frac{T_n}{T} = \left(\frac{p_n}{p'}\right)^{\frac{\gamma-1}{\gamma}}$$

therefore

$$\frac{A}{A_s} = \frac{(p_s/p')^{\frac{1}{\gamma}} \sqrt{1 - (p_s/p')^{\frac{\gamma-1}{\gamma}}}}{(p_n/p')^{\frac{1}{\gamma}} \sqrt{1 - (p_n/p')^{\frac{\gamma-1}{\gamma}}}}$$

This equation defines the relation between p'/p_n and p_s/p_n. The static pressure at the nozzle, p_n, is equal to

$$\left(\frac{2}{\gamma + 1}\right)^{\frac{\gamma}{\gamma-1}} p'$$

when the flow through the nozzle is acoustic and is equal to atmospheric pressure when the flow is not acoustic. The equation must be solved graphically for p'.

APPENDIX III

Comparison of Gain in Jet Thrust Horsepower with Loss in Engine Power for Nozzle Areas Less Than Critical

In the region where reduction in nozzle size causes a loss in engine power, the gain in net thrust is given by

$$\Delta \text{ thp} = \eta_p(P - P_o) + \frac{M_e \bar{V}_e V_o}{550}$$

where P_o is the brake horsepower for the case of the unrestricted exhaust stack at the same operating conditions and P is the brake horsepower with the constricted nozzle. But

$$\frac{P - P_o}{I_o} \quad \frac{I - I_o}{I_o} \quad \frac{\Delta \phi}{\phi_o}$$

Therefore

$$\frac{\Delta \text{ thp}}{I_o} = \eta_p \frac{\Delta \phi}{\phi_o} + K \bar{V}_e$$

where

$$K = \frac{M_e V_o}{550 I_o}$$

$$\frac{p_s A_s V_s}{R_c T_s} = \frac{p_n A V_n}{R_c T_n}$$

where

A_s stack area

p_s stack pressure

V_s corresponding velocity

T_s corresponding temperature

If it is assumed that no heat is lost from the stack to the nozzle, the principle of the conservation of energy gives:

$$V_s^2 = (T - T_s) \frac{2\gamma}{\gamma - 1} R_c$$

$$V_n^2 = (T - T_n) \frac{2\gamma}{\gamma - 1} R_c$$

The continuity equation becomes

$$\frac{p_s A_s \sqrt{T - T_s}}{T_s} = p_n A \frac{\sqrt{T - T_n}}{T_n}$$

But

$$\frac{T_s}{T} = \left(\frac{p_s}{p'}\right)^{\frac{\gamma-1}{\gamma}}$$

and

$$\frac{T_n}{T} = \left(\frac{p_n}{p'}\right)^{\frac{\gamma-1}{\gamma}}$$

therefore

$$\frac{A}{A_s} = \frac{(p_s/p')^{\frac{1}{\gamma}} \sqrt{1 - (p_s/p')^{\frac{\gamma-1}{\gamma}}}}{(p_n/p')^{\frac{1}{\gamma}} \sqrt{1 - (p_n/p')^{\frac{\gamma-1}{\gamma}}}}$$

This equation defines the relation between p'/p_n and p_s/p_n. The static pressure at the nozzle, p_n, is equal to

$$\left(\frac{2}{\gamma + 1}\right)^{\frac{\gamma}{\gamma-1}} p'$$

when the flow through the nozzle is acoustic and is equal to atmospheric pressure when the flow is not acoustic. The equation must be solved graphically for p'.

APPENDIX III

Comparison of Gain in Jet Thrust Horsepower with Loss in Engine Power for Nozzle Areas Less Than Critical

In the region where reduction in nozzle size causes a loss in engine power, the gain in net thrust is given by

$$\Delta \text{ thp} = \eta_p(P - P_o) + \frac{M_o \bar{V}_e V_o}{550}$$

where P_o is the brake horsepower for the case of the unrestricted exhaust stack at the same operating conditions and P is the brake horsepower with the constricted nozzle. But

$$\frac{P - P_o}{I_o} \quad \frac{I - I_o}{I_o} \quad \frac{\Delta \phi}{\phi_o}$$

Therefore

$$\frac{\Delta \text{ thp}}{I_o} = \eta_p \frac{\Delta \phi}{\phi_o} + K \bar{V}_e$$

where

$$K = \frac{M_o V_o}{550 I_o}$$

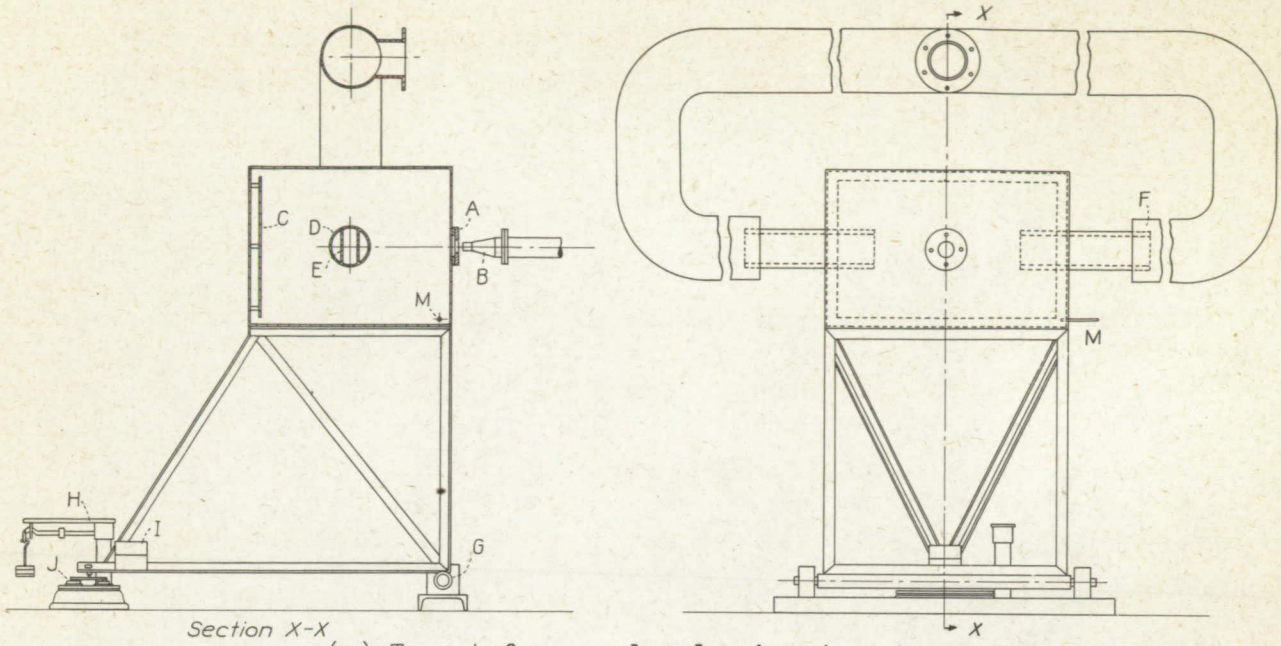

(a) Target for sea level exhaust pressure

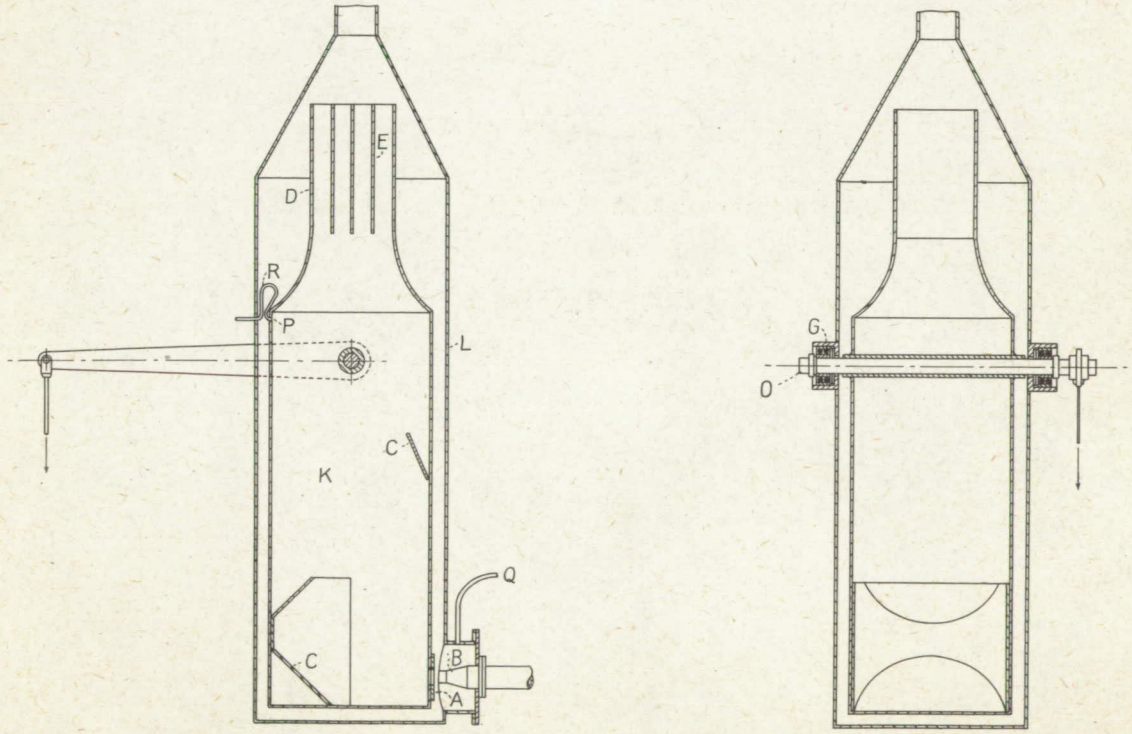

(b) Target for altitude exhaust pressure

Figure 1.- Diagram of thrust measuring device.

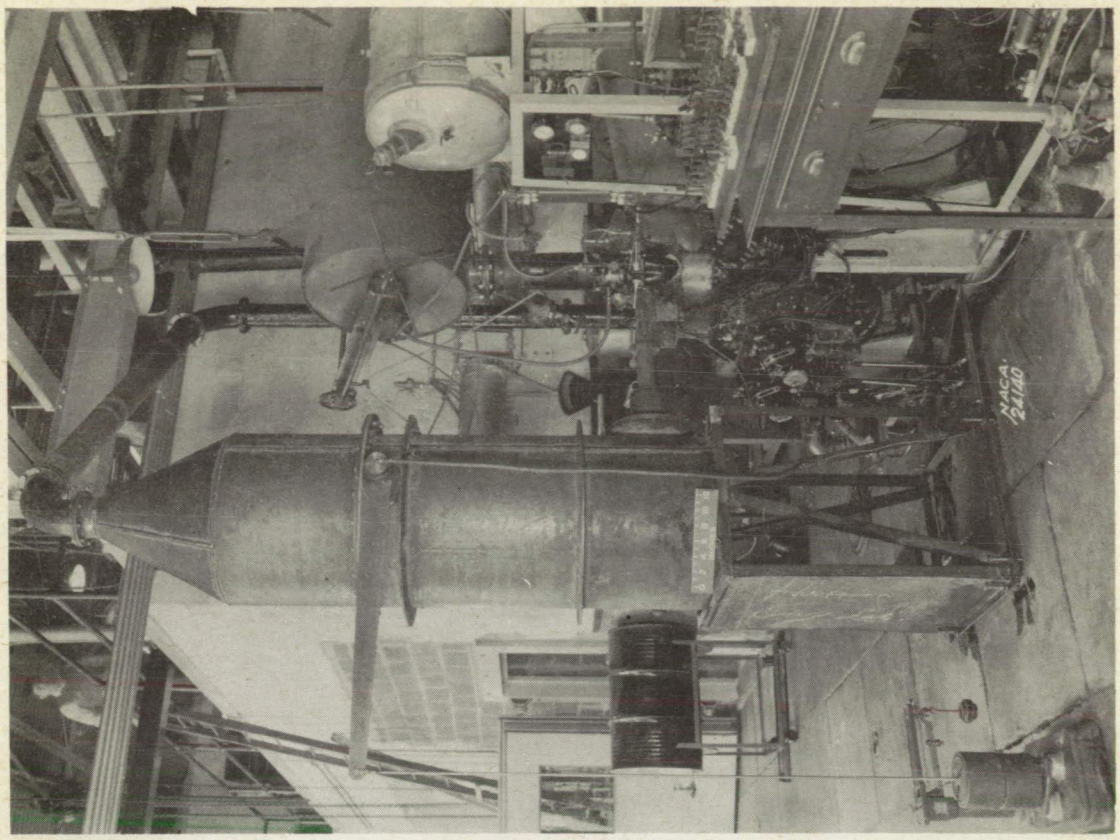

ure 2b.- Test set-up for altitude exhaust pressure.

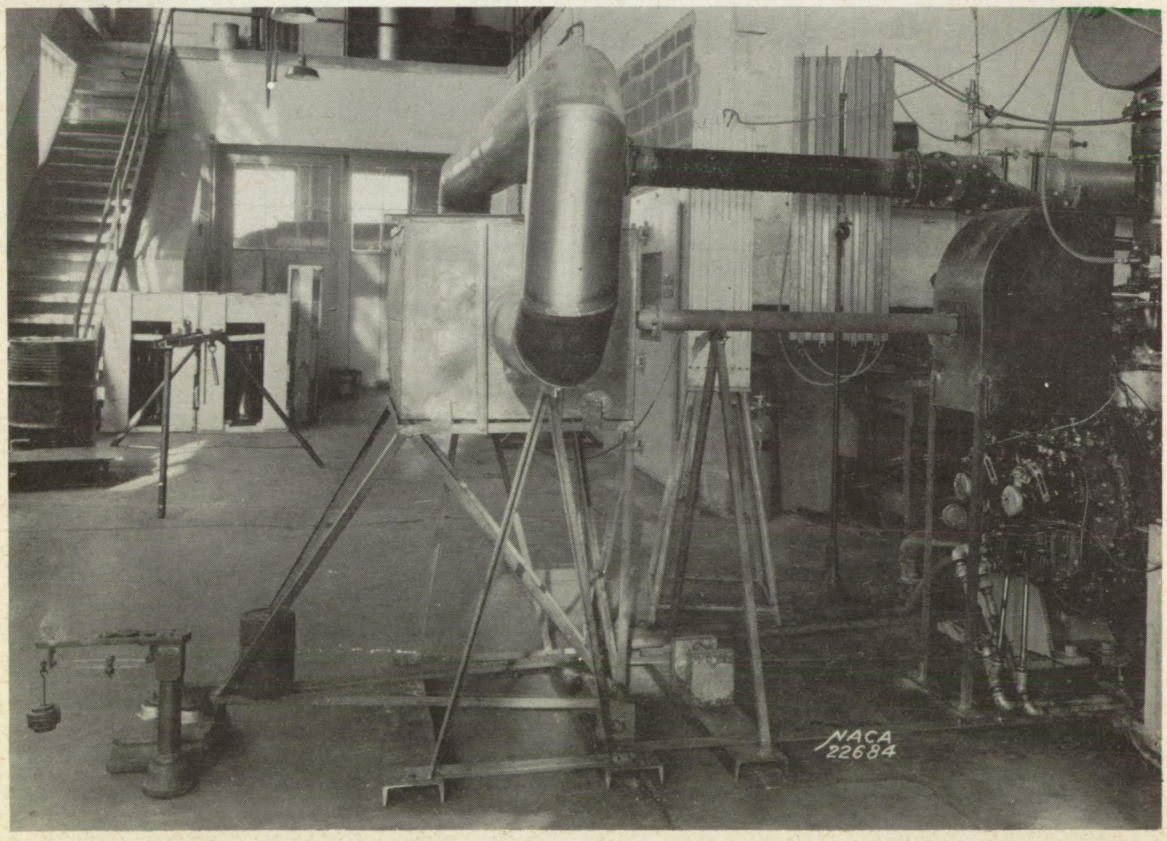

Figure 2a.- Test set-up for sea-level exhaust pressure.

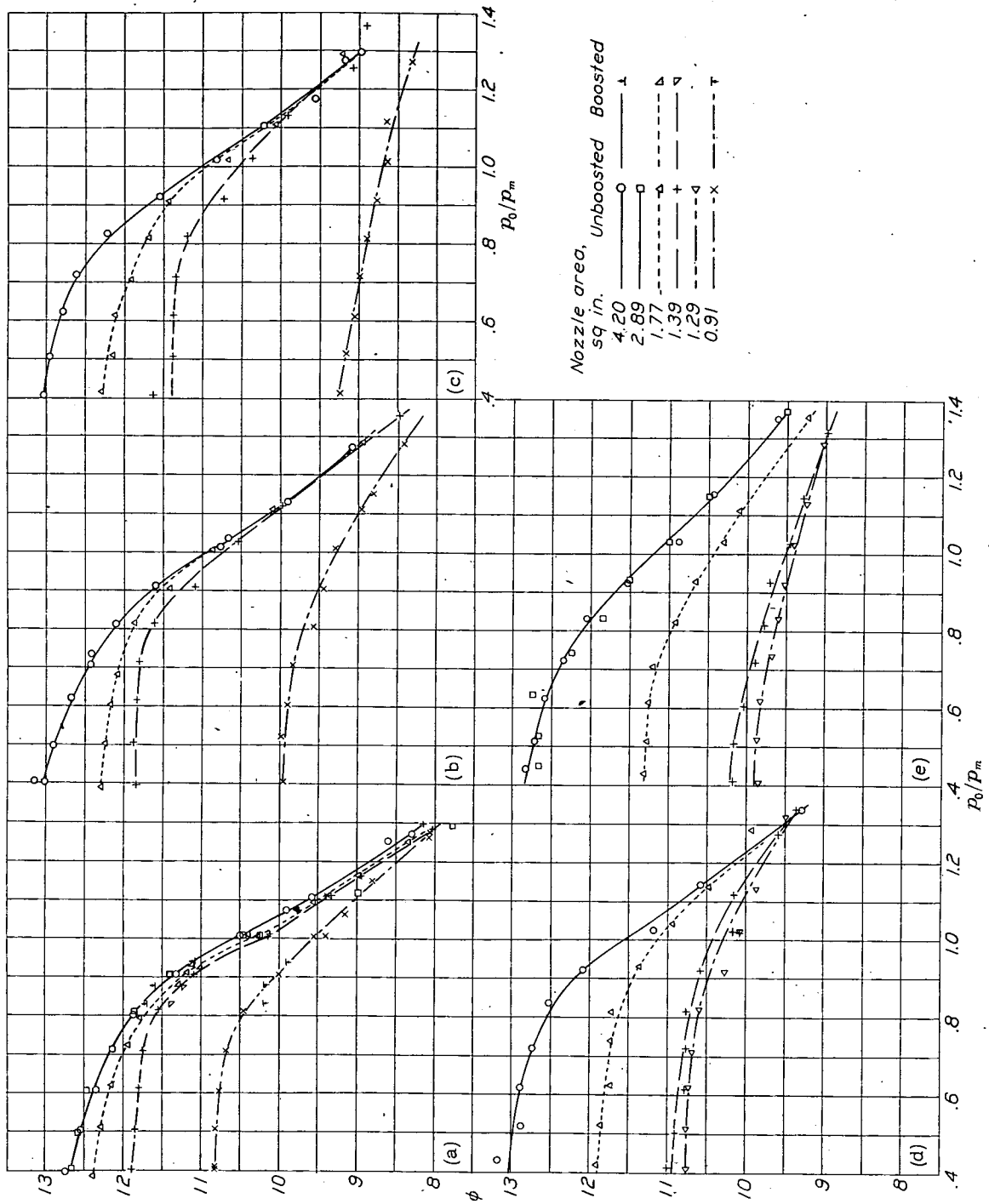

Engine speed, rpm

(a) 1300

(b) 1500

(c) 1700

(d) 1900

(e) 2100

Figure 3.- Variation of ϕ with p_0/p_m and nozzle area.

Engine speed, rpm

(a) 1300

(b) 1500

(c) 1700

(d) 1900

(e) 2100

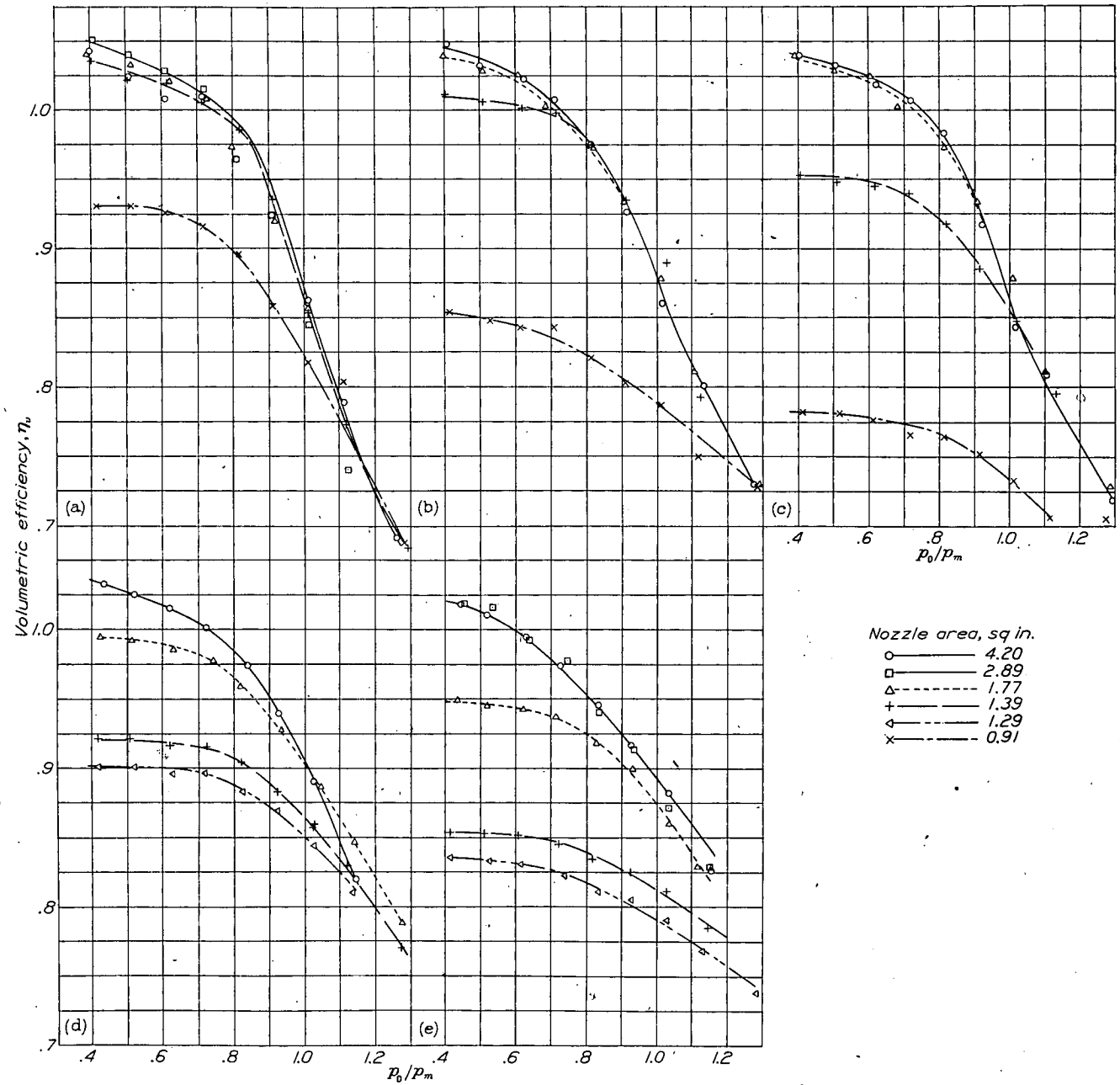

Figure 4.- Variation of volumetric efficiency, η_v, with p_0/p_m and nozzle area.

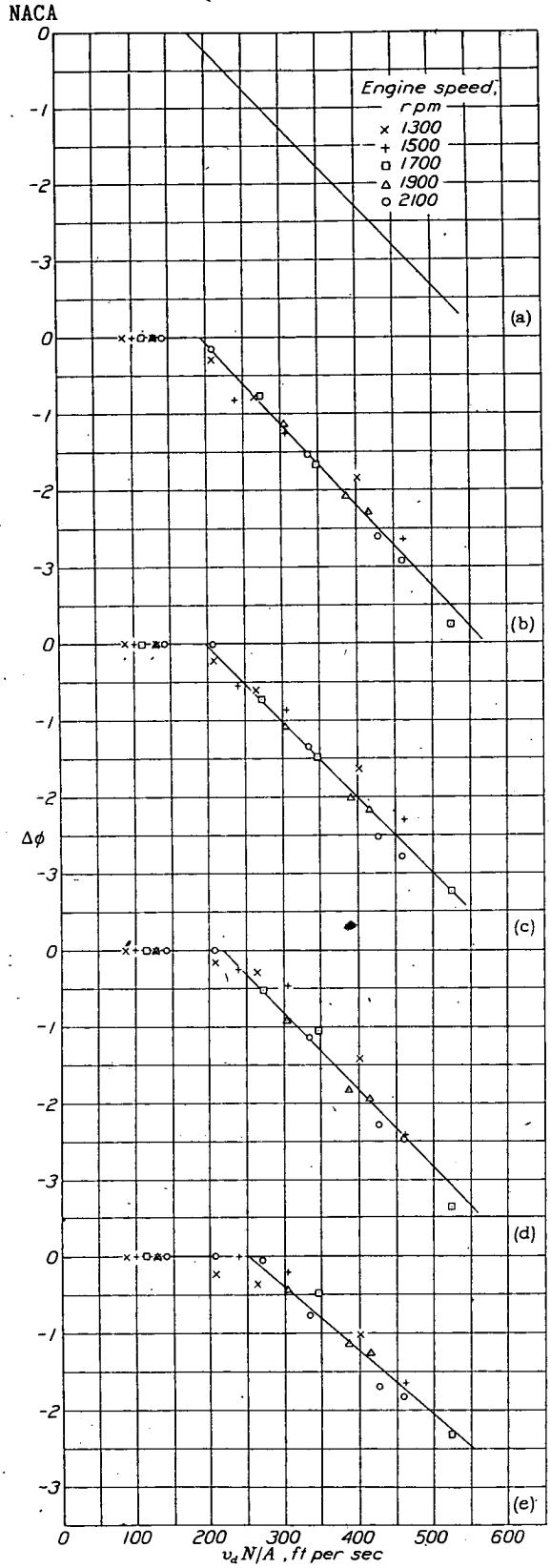

(a) p_o/p_m=0.2;(b) p_o/p_m=0.4;(c) p_o/p_m=0.6;
(d) p_o/p_m=0.8;(e) p_o/p_m=1.0.

Figure 5.- Variation of $\Delta\phi$ with $v_d N/A$.

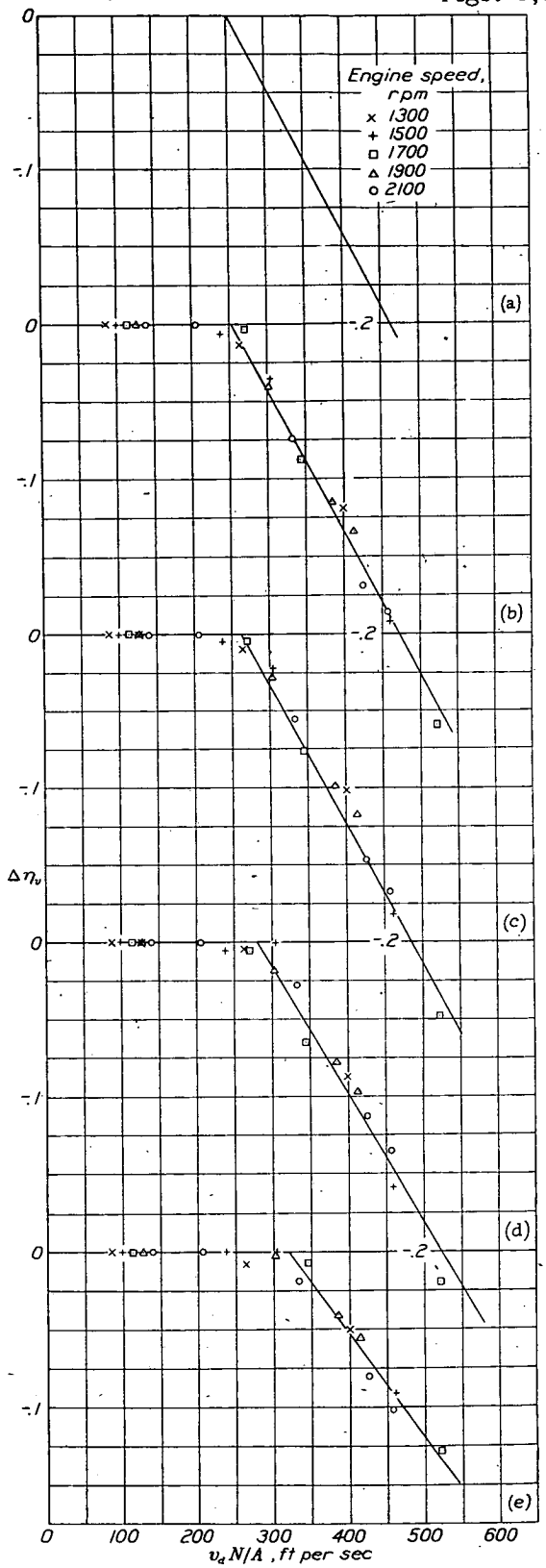

(a) p_o/p_m=0.2;(b) p_o/p_m=0.4;(c) p_o/p_m=0.6;
(d) p_o/p_m=0.8;(e) p_o/p_m=1.0.

Figure 6.- Variation of $\Delta\eta_v$ with $v_d N/A$.

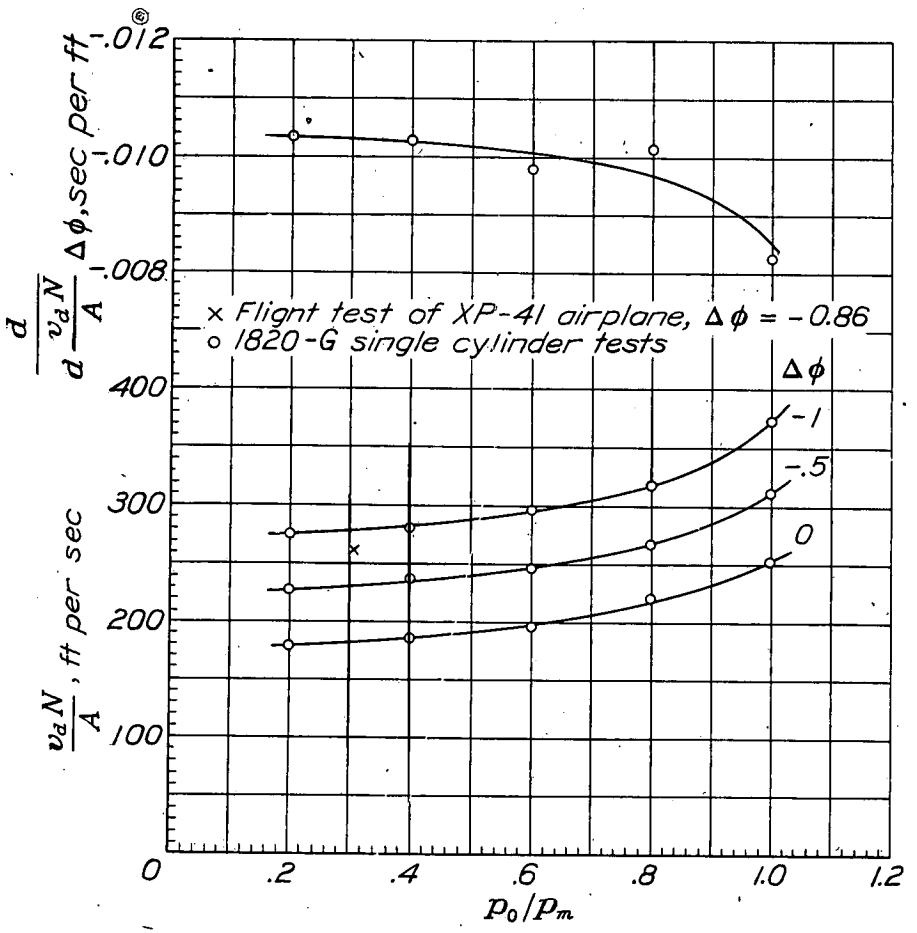

Figure 7.- Variation of $v_d N/A$ and $d(\Delta\phi)/d(v_d N/A)$ with p_o/p_m.

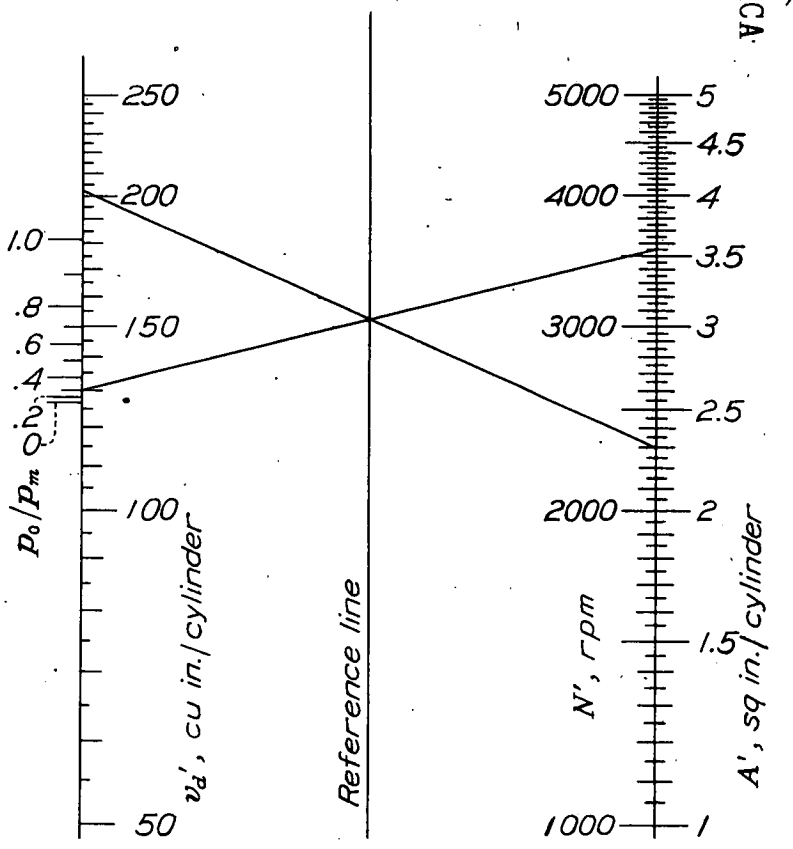

Figure 8.- Nomogram for determining optimum nozzle area.

Figs. 7, 8

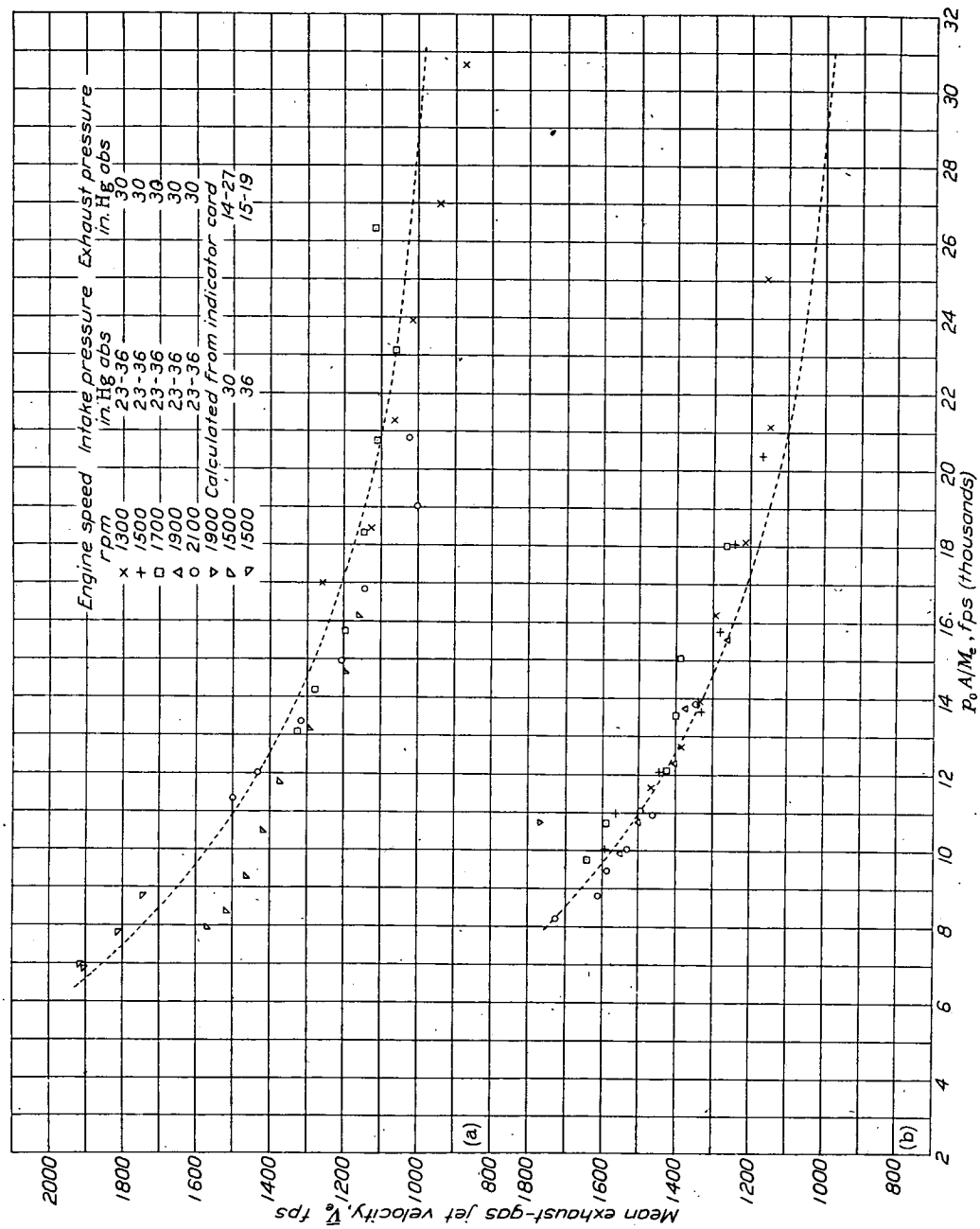

(a) Nozzle area, 4.20 sq in. (b) Nozzle area, 2.85 sq in.

Figure 9a to e.- Variation of mean effective exhaust-gas jet velocity, $\bar{V}_e$, with p_0A/M_e.

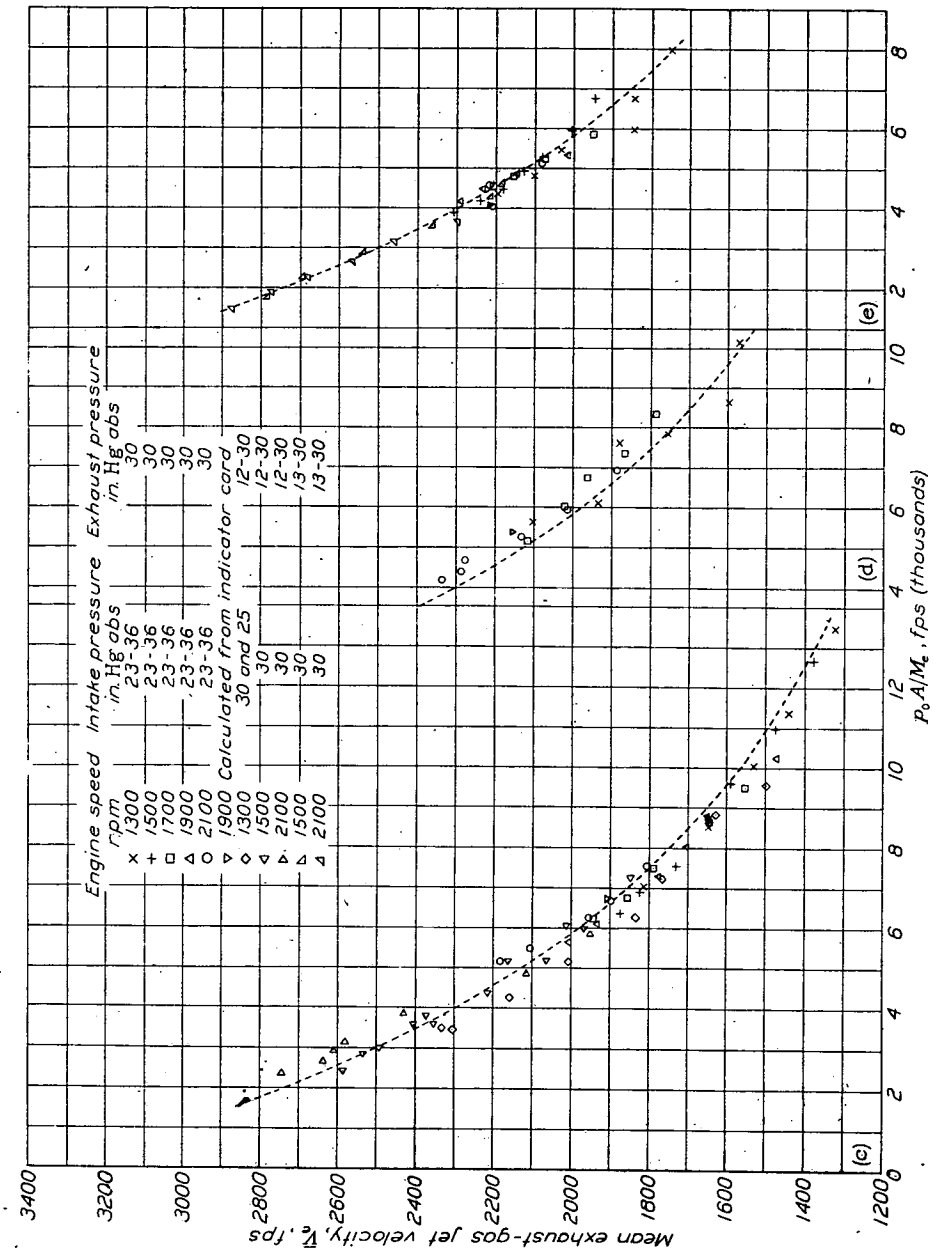

(c) Nozzle area, 1.77 sq in. (d) Nozzle area, 1.39 sq in. (e) Nozzle area, 0.91 sq in.

Figure 9.- Concluded.

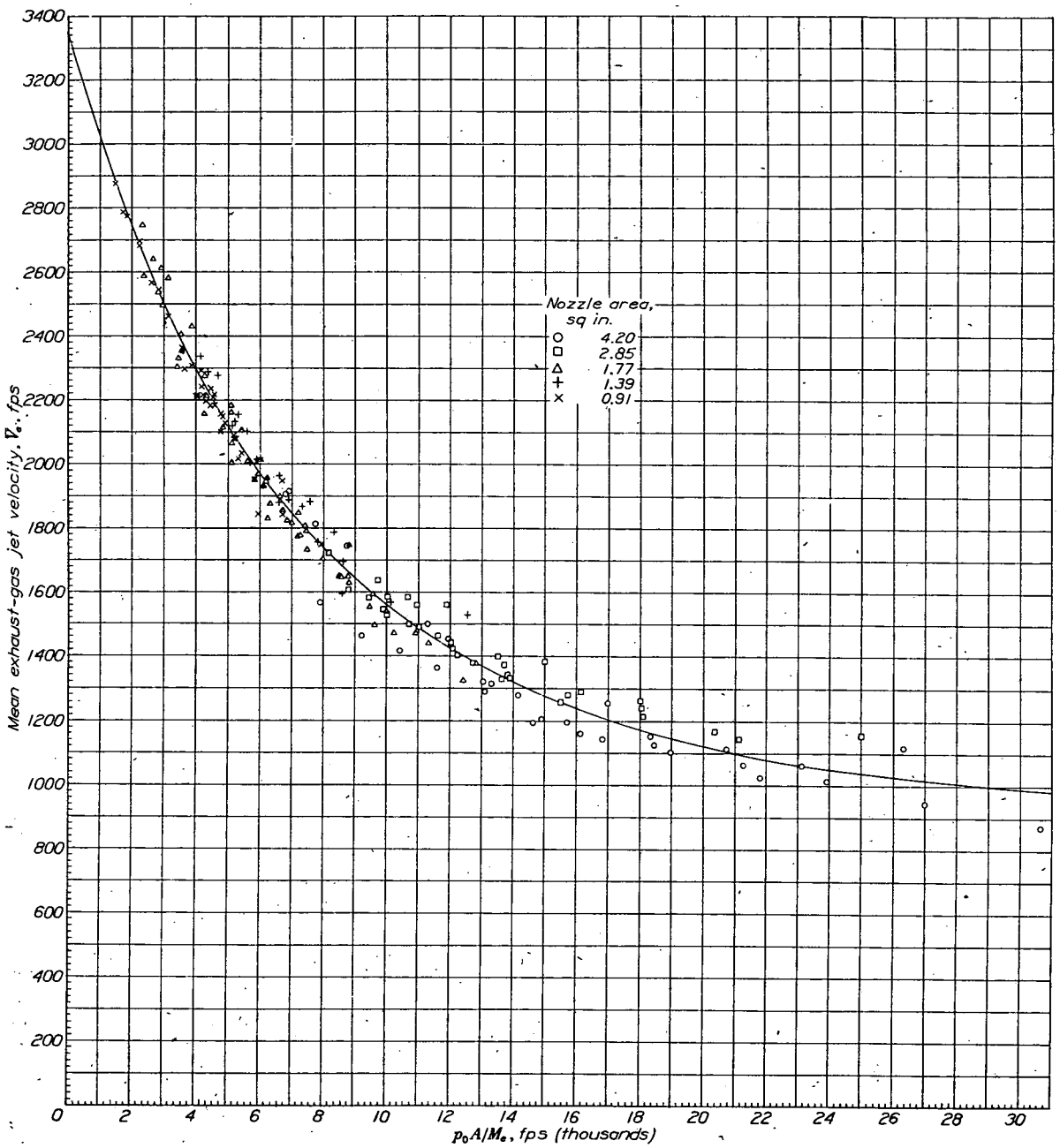

Figure 10.- Correlation of all data on variation of mean effective exhaust-gas jet velocity, $\bar{V}_e$, with p_0A/M_e

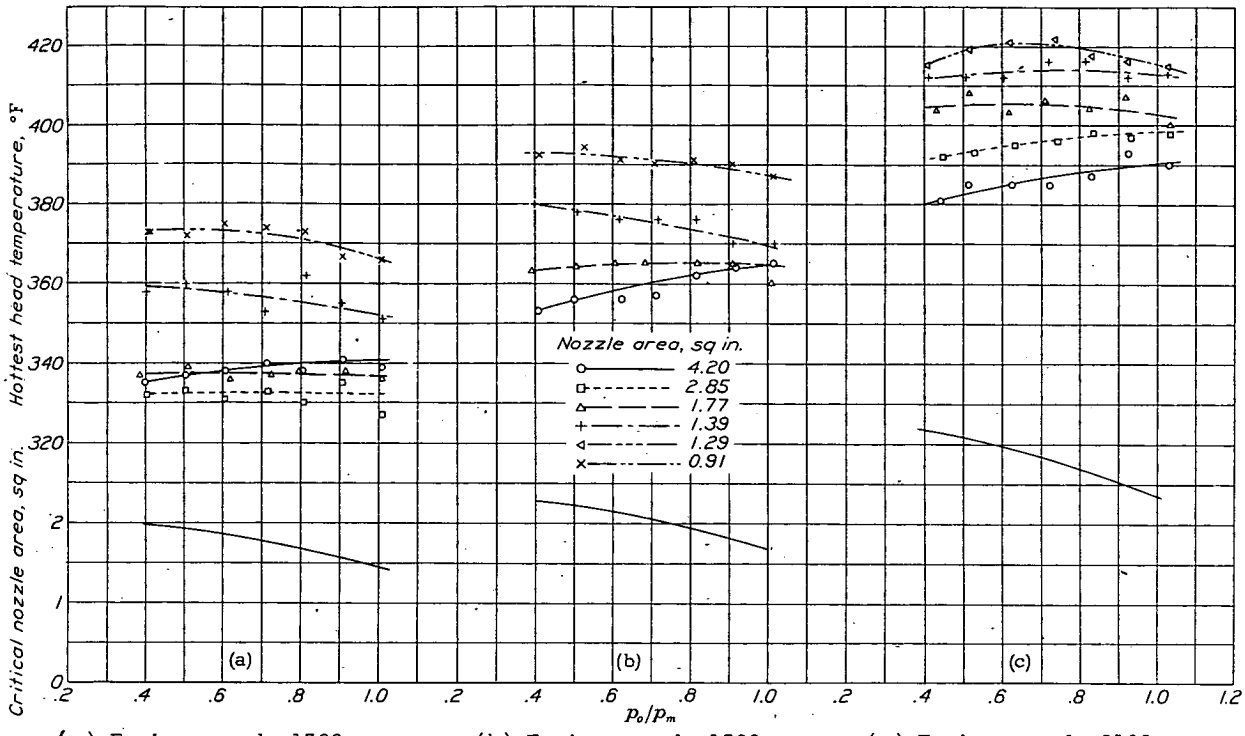

(a) Engine speed, 1300 rpm. (b) Engine speed, 1500 rpm. (c) Engine speed, 2100 rpm.

Figure 13.- Effect of nozzle area on cylinder-head temperature(p_m = 30 in. Hg abs).

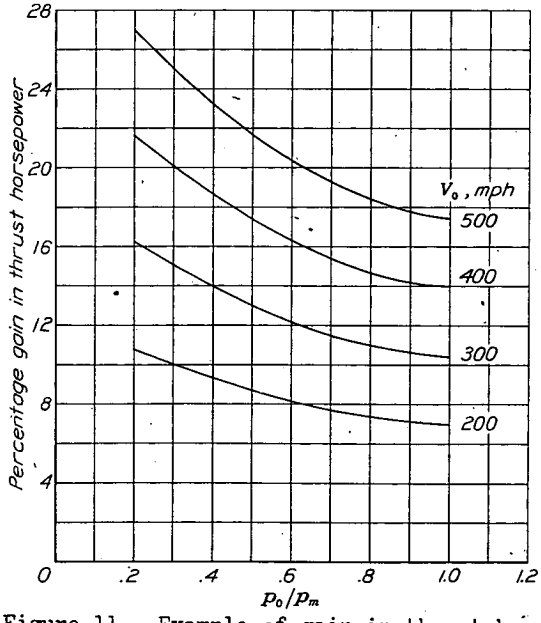

Figure 11.- Example of gain in thrust hp with exhaust-gas jet propulsion with optimum $v_d N/A$. (Weight of exhaust gas, 0.002 lb per sec per bhp; η_v taken from fig. 4e ; η_p = 0.85)

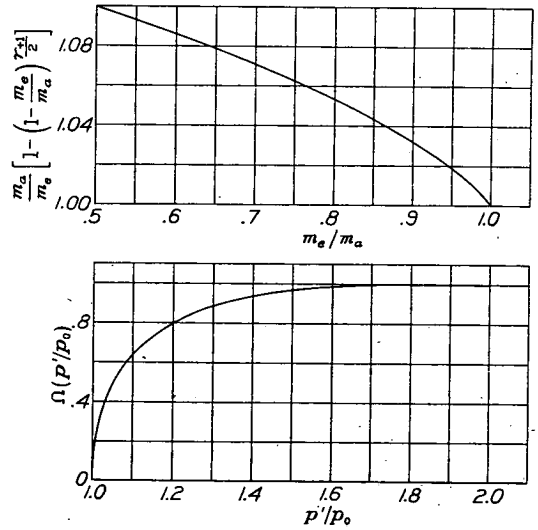

Figure 14.- Values of the functions

$$\frac{m_a}{m_e}\left[1-\left(1-\frac{m_e}{m_a}\right)^{\frac{\gamma-1}{2}}\right]$$

and $\Omega(p'/p_o)$ for γ=1.3.

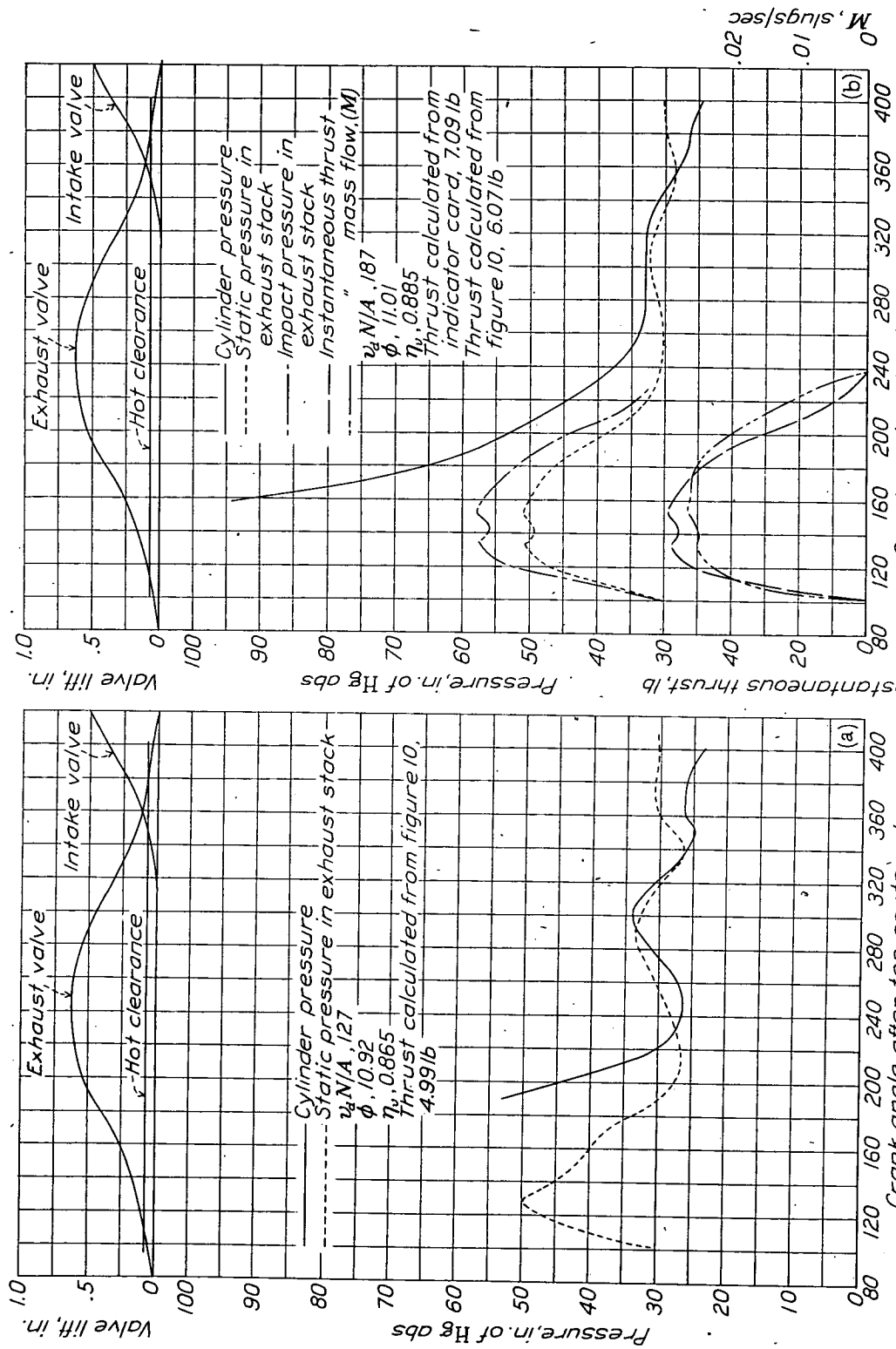

Figure 12a to f.- Effect of nozzle area on pressure-time diagram in the cylinder and exhaust stack and on the rate of exhaust discharge(Engine speed, 1900 rpm, sea-level exhaust and inlet manifold pressure, fuel-air ratio, 0.08.)

(a) Nozzle area, 4.20 sq in.

(b) Nozzle area, 2.85 sq in.

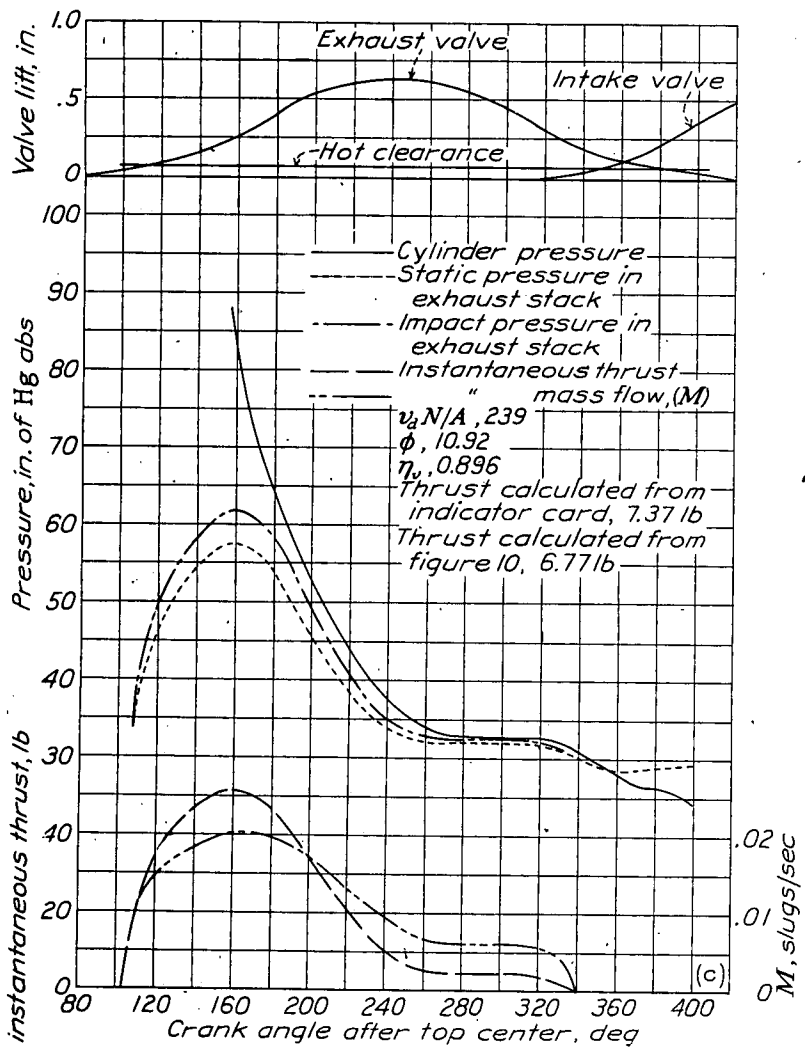

(c) Nozzle area, 2.24 sq in.

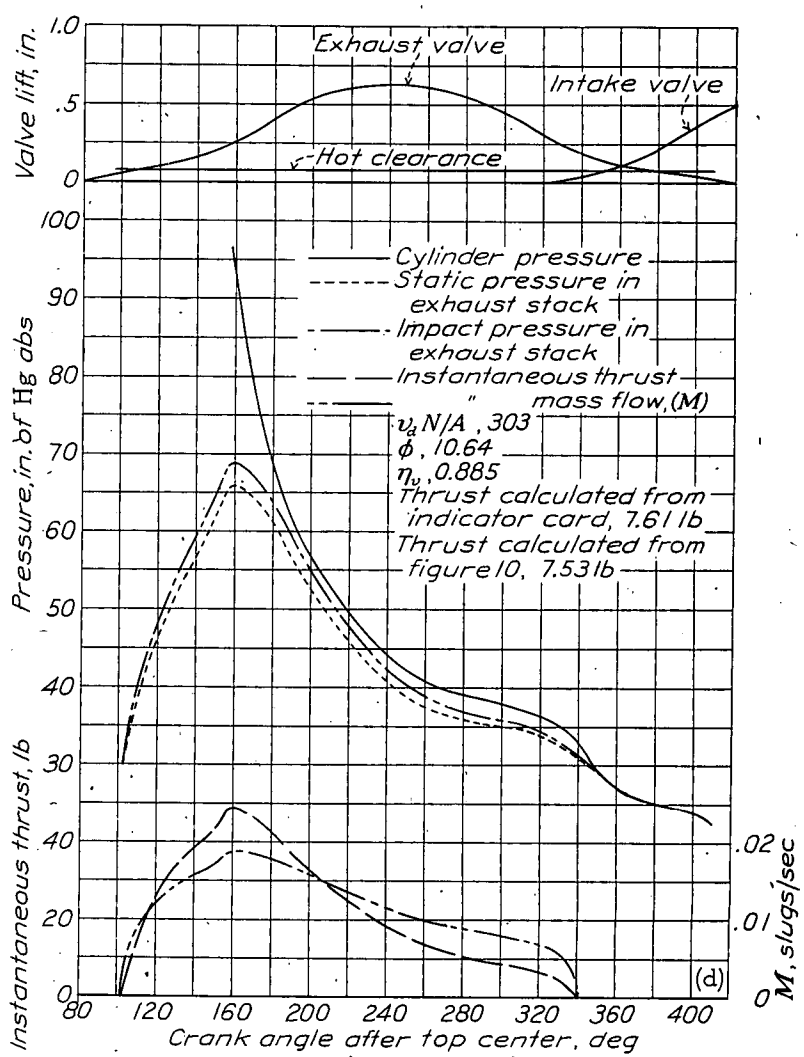

(d) Nozzle area, 1.77 sq in.

Figure 12.- Continued.

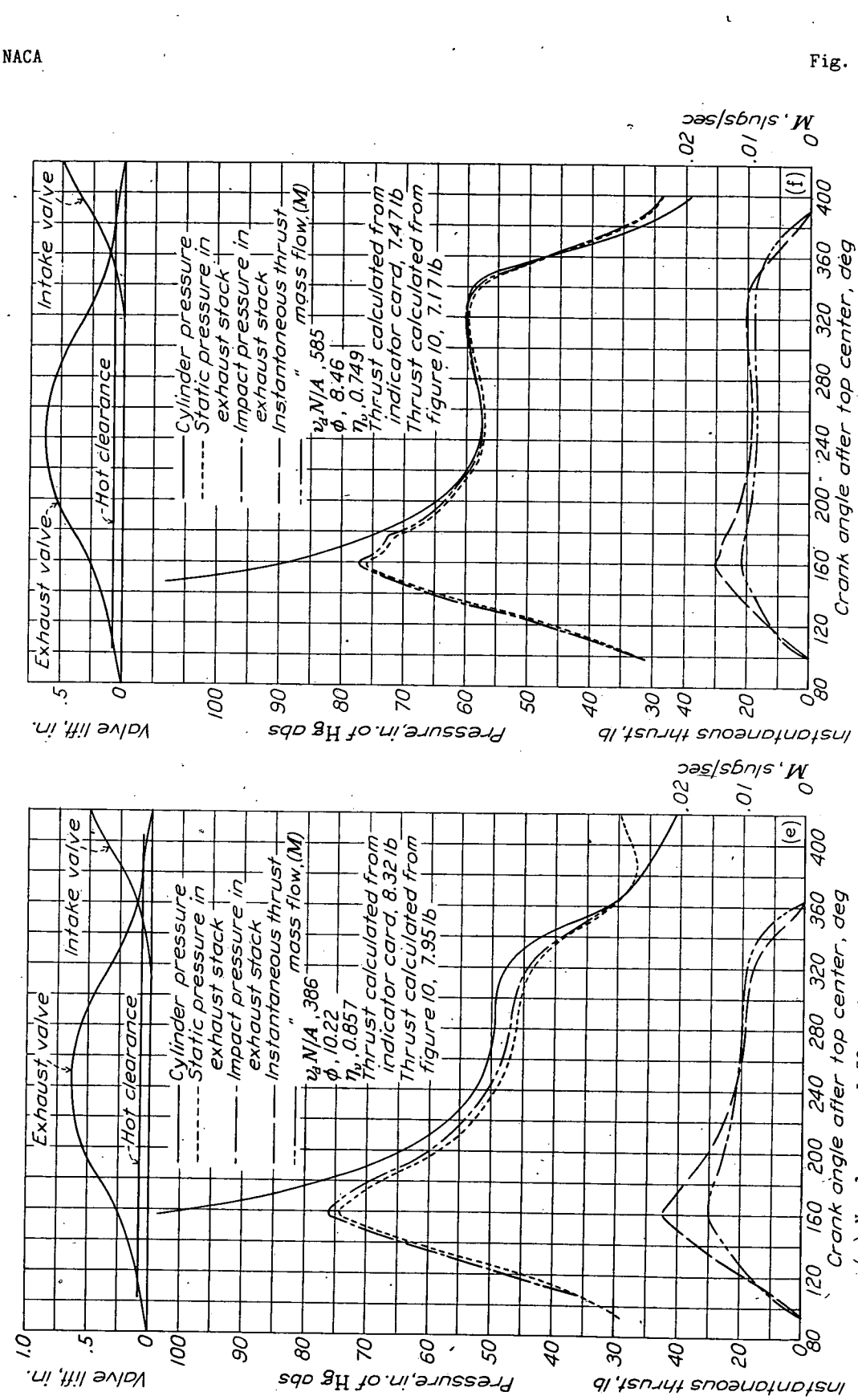

(e) Nozzle area, 1.39 sq in.

(f) Nozzle area, 0.91 sq in.

Figure 12.- Concluded.